Paper I

scientific reports

Check for updates

OPEN

The microbial composition of the initial insult can predict the prognosis of experimental sepsis

Szabolcs Péter Tallósy[1,3], Marietta Zita Poles[1,3], Attila Rutai[1], Roland Fejes[1], László Juhász[1], Katalin Burián[2], József Sóki[2], Andrea Szabó[1], Mihály Boros[1] & József Kaszaki[1]✉

We hypothesized that the composition of sepsis-inducing bacterial flora influences the course of fecal peritonitis in rodents. Saline or fecal suspensions with a standardized dose range of bacterial colony-forming units (CFUs) were injected intraperitoneally into Sprague–Dawley rats. The qualitative composition of the initial inoculum and the ascites was analyzed separately by MALDI-TOF mass spectrometry. Invasive monitoring was conducted in separate anesthetized groups (n = 12–13/group) after 12, 24, 48 and 72 h to determine rat-specific organ failure assessment (ROFA) scores. Death and ROFA scores peaked at 24 h. At this time, 20% mortality occurred in animals receiving a monomicrobial *E. coli* suspension, and ROFA scores were significantly higher in the monomicrobial subgroup than in the polymicrobial one (median 6.5; 5.0–7.0 and 5.0; 4.75–5.0, respectively). ROFA scores dropped after 48 h, accompanied by a steady decrease in ascites CFUs and a shift towards intra-abdominal monomicrobial *E. coli* cultures. Furthermore, we found a relationship between ascites CFUs and the evolving change in ROFA scores throughout the study. Hence, quantitatively identical bacterial loads with mono- or polymicrobial dominance lead to a different degree of sepsis severity and divergent outcomes. Initial and intraperitoneal microbiological testing should be used to improve translational research success.

Experimental models can provide a basis for the development of human therapeutics, but an effective laboratory strategy cannot always be transferred to clinical practice. The most recent Minimum Quality Threshold in Preclinical Sepsis Studies (MQTiPSS) criteria outline the recommended scheme for rodent experimental sepsis[1] and highlight the importance of consecutive evaluation of established signs of organ failure, similarly to the sequential organ failure assessment (SOFA) scoring systems in humans[2,3]. Nevertheless, findings of preclinical laboratory studies are still difficult to compare[4], because the magnitude of bacterial load is problematic to standardize and the composition of the intraluminal microbiome at the time of the infection is usually unidentified; the impact of the microbial profile on the progression of events therefore also remains unknown[5].

The bacterial strains of human or rat stool are broadly representative of the principally polymicrobial flora of the distal colon, and therefore intra-abdominal administration of fecal matter is considered a good rodent model for human peritonitis-linked sepsis. Among the many CLP alternatives[6], fecal slurries, intra-abdominal injections of fresh or stored solutions of fecal suspensions, can reduce the inherent variance of invasive surgical procedures[7]. Nevertheless, the composition and activity of competing microbial communities may vary greatly even in precisely quantified fecal doses; the results can therefore also be biased when concise qualitative information on the invading microorganisms is lacking[8]. The question of whether a dominant strain or certain strains collectively—a single component or a multicultural microbial community—will determine the initial severity and the natural course of bacterial sepsis remains unresolved.

Based on this knowledge gap, we hypothesized that the unknown qualitative bacterial composition within the fecal mass triggering the insults could be a highly important confounding factor and a decisive descriptor of the course of a septic scenario. Therefore, our primary aim was to investigate the relationship between the bacterial concentration and the qualitative composition of a standardized fecal suspension and the severity of the

[1]Institute of Surgical Research, Albert Szent-Györgyi Medical School, University of Szeged, Szeged, Hungary. [2]Department of Medical Microbiology, Albert Szent-Györgyi Health Center and Faculty of Medicine, University of Szeged, Szeged, Hungary. [3]These authors contributed equally: Szabolcs Péter Tallósy and Marietta Zita Poles. ✉email: kaszaki.jozsef@med.u-szeged.hu

progressively evolving experimental sepsis as a function of time. To this end, we have used a qualitative, murine-specific sickness scoring system, and we have developed a comprehensive, MQTiPSS-compatible evaluation of organ function parameters to adequately quantify the clinical condition of the septic animals with a rat-specific organ failure assessment (ROFA) scoring system[9] between 12 and 72 h after induction.

Furthermore, it has been shown that *E. coli* strains alone can lead to fulminant sepsis with high early mortality, while a combination of *E. coli* and other bacterial strains results in the development of a more localized process with intra-abdominal abscess formation[7,10]. Although *E. coli* strains are the most abundant facultative aerobes in the intestines, there are numerous other Gram-negative and Gram-positive pathogens in the microflora that are potentially responsible for gastrointestinal tract-derived sepsis. Fecal infections are generally considered polymicrobial, but the question of whether *E. coli* or other dominant strains of the fecal matter influence the initial severity of sepsis is unresolved. Our second objective was thus to retrospectively analyze the influence of bacterial background on the initial severity and outcome of fecal peritonitis.

Indeed, intra-abdominal sepsis is a dynamic condition involving potentially destructive events when the pro-inflammatory process trespasses the peritoneal cavity and several lines of host defense to eliminate the insult[11]. We therefore hypothesized that changes in intra-abdominal microbial diversity (and the fate of individual members of a microbial community ecosystem) may play a key role in determining sepsis progression since the peritoneal environment and intraperitoneal immunological processes are thought to influence not only the concentration but also the composition of the bacterial culture present in the ascites. Hence, our third objective was to determine the variation of the composition and the change of germ counts of the bacterial populations in the abdominal cavity as a function of time.

Along these lines, we tracked time-dependent changes in the composition of intra-abdominal strains in model experiments with standardized and characterized bacterial load. We have demonstrated that the microbial community structure of the insult may critically influence the course and consequences of bacterial sepsis in laboratory rats. We propose that qualitative, microbiology-based screening should be properly integrated into the design of in vivo sepsis models.

Results

Animal well-being and mortality. Intra-abdominal sepsis was induced by fecal inoculum with known colony forming units (CFUs). Assessments of animal well-being (using a rat-specific, well-being-related sickness score, RSS) and organ dysfunction (using the rat-specific ROFA scoring system, see later) were performed, while the termination of each experiment was scheduled at predetermined time points (12 h, 24 h, 48 h and 72 h) after sepsis induction (Fig. 1a). The rat-specific RSS score did not change significantly at 6 h and 12 h after the septic challenge (Fig. 1b), and there was no mortality in these groups (Fig. 1c). Within nearly 24 h, the condition of some septic animals deteriorated significantly, the RSS values having reached a critical value of 6 (i.e. the threshold for a humane endpoint) and therefore n = 3, n = 4 and n = 3 animals were humanely euthanized in Groups 24 h, 48 h and 72 h, respectively. The number of euthanized animals (the underlying rationale is discussed in the "Materials and methods" section) is included in mortality calculations (Fig. 1c). The general condition of surviving septic animals did not deteriorate between 48 and 72 h, as reflected by RSS scores of less than 2 without further lethality (Fig. 1b).

Inflammatory biomarkers. We determined the plasma levels of interleukin-6 (IL-6; a relatively early biomarker in sepsis) and endothelin-1 (ET-1; a marker of tissue hypoxia) to confirm and characterize the course of pro-inflammatory processes in the animals. Elevated levels of plasma IL-6 were observed 12 h after induction ($P = 0.018$); plasma ET-1 concentration increased significantly at 24 h of sepsis (Fig. 2). Thereafter, levels of both biomarkers returned to those of the sham-operated animals.

Circulatory and subcellular oxygen dynamics. To assess the sepsis-induced tissue hypoperfusion, we determined the systemic oxygen extraction rate (OER) and the efficacy of mitochondrial respiration (from liver biopsies) in sham-operated and septic animals with different observation periods. There was no significant difference in the OER between the sham-operated and septic animals 12 h after septic insult, but the values showed a significant reduction after 24 h of sepsis (Fig. 3a). In sepsis groups with longer observation, less diminished OER values were detected. The Complex II-linked capacity of oxidative phosphorylation—indicative of subcellular oxygen consumption—also shows deterioration in the 24 h septic animals only ($P < 0.01$ vs sham-operated) (Fig. 3b).

Changes in ROFA score components. The cumulative value of the ROFA score showed significant increases at 24 and 48 h (Fig. 4). Deteriorations in 24 h values were attributable to all parameters examined, whereas similar changes were also present for most parameters at 48 h, except for the significantly not different blood lactate and plasma ALT values. ROFA scores returned to the values of sham-operated animals after 72 h.

Retrospective analyses

Microbial features of the fecal inoculum and the ascites. In addition to determining the CFUs, analysis of the bacterial pattern (by MALDI-TOF mass spectrometry) was performed from both the sepsis-inducing fecal inocula and the ascites (the latter taken upon termination of the experiments in Grs. 12–72 h). This retrospective qualitative microbiological analysis (48 h after induction) revealed that, despite the statistically similar bacterial doses (Fig. 5), marked qualitative differences (e.g. in bacterial composition and monomicrobial/polymicrobial pattern) existed in the composition of the inocula (Table 1, Supplementary Material S2, Supplementary Table S1). It was proven that only *E. coli* was present in 20% of inocula ($n\Sigma = 10$) and all early (24-h) sepsis

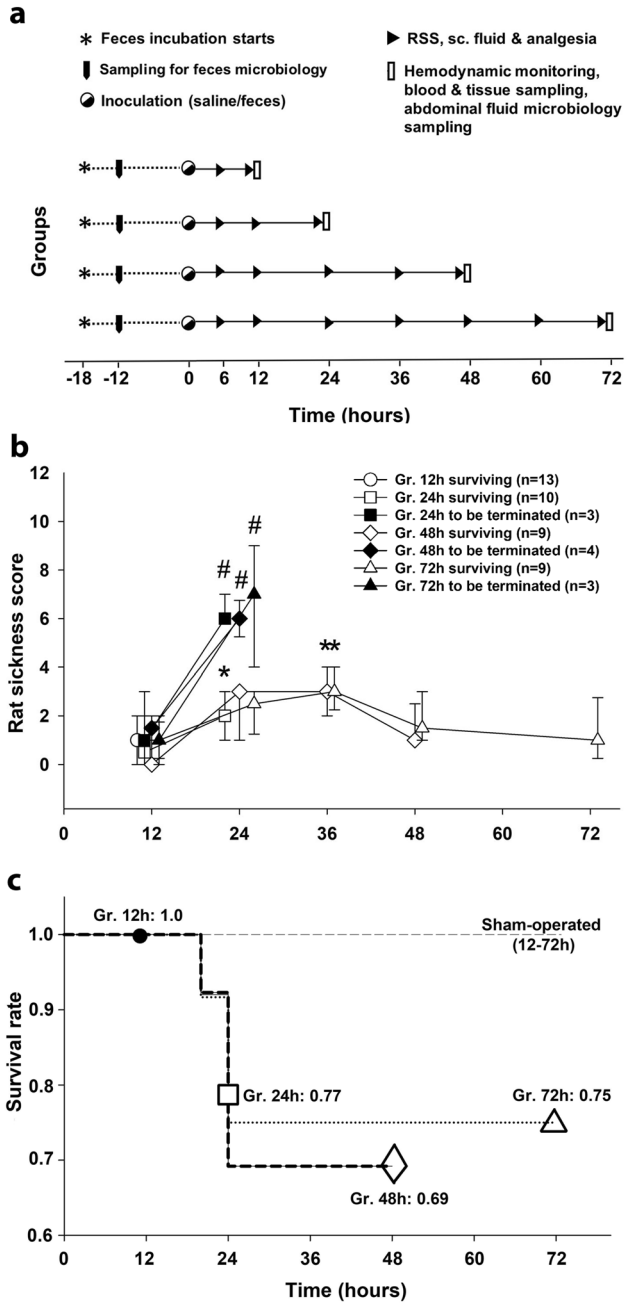

Figure 1. Experimental protocol, rat-specific sickness score (RSS) and mortality at different stages of the sepsis. **(a)** The scheme for the experimental protocol (groups, interventions and assessments). The animals were randomly assigned to sham-operated and septic groups, which were further divided into four independent groups each according to the termination timeline set between 12 and 72 h. Interventions and assessments (including RSS score) are marked with symbols. The animals were injected with an inoculum fitting the 1.02×10^6–5.6×10^6 CFU range. This dosing regimen caused marked RSS changes and organ dysfunction leading to approximately 20% mortality in a pilot study (see Supplementary Material S1). **(b)** Within the cohort of septic animals, RSS score values of surviving animals (open symbols) and those reaching the threshold value of 6 (euthanized subjects; black symbols) are shown separately (*Grs.* groups). Plots demonstrate the median values and the 25th (lower whisker) and 75th (upper whisker) percentiles. Within groups: Friedman test and Dunn's post-hoc test. $^{*}P < 0.05$ vs value of non-lethal 12 h sepsis. Between groups: Mann–Whitney U test. $^{\#}P < 0.05$ lethal vs non-lethal sepsis at 24 h. **(c)** Kaplan–Meier survival analysis performed on the four sepsis groups (Grs. 12 h, 24 h, 48 h and 72 h) and four sham-operated groups; survival rates are indicated.

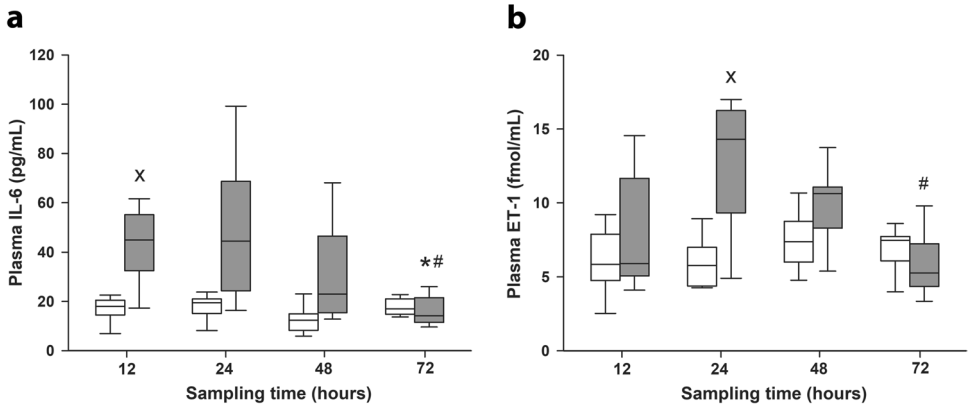

Figure 2. Plasma interleukin 6 (IL-6) **(a)** and endothelin-1 (ET-1) concentrations **(b)** in sham-operated animals (n = 12–13, white boxes) and in the different sepsis groups representing different stages of sepsis (grey boxes). The number of animals used in the various sepsis groups is indicated in Table 1. Plots demonstrate the median (horizontal line in the box) and the 25th (lower whisker) and 75th (upper whisker) percentiles. A comparison between groups was conducted with the Kruskal–Wallis test followed by Dunn's post-hoc test. $^{X}P < 0.05$ vs sham-operated groups; $^{*}P < 0.05$ vs 12 h sepsis (between sepsis groups); $^{\#}P < 0.05$ vs 24 h sepsis (between sepsis groups).

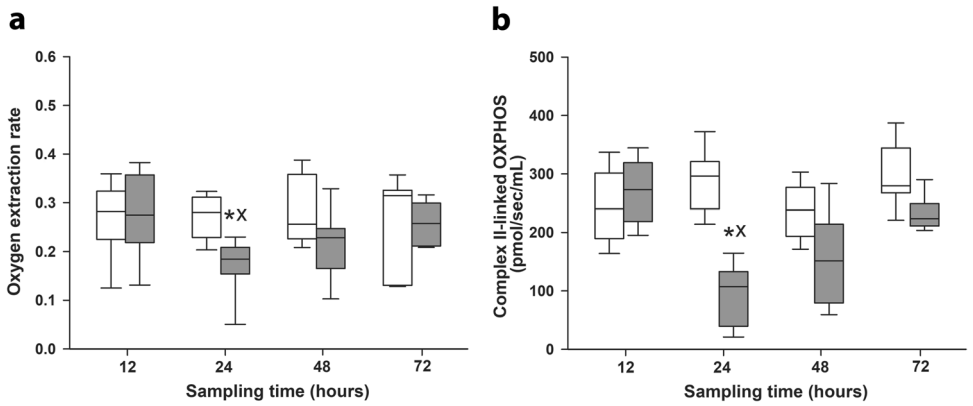

Figure 3. Oxygen extraction rate **(a)** and mitochondrial respiration **(b)** in sham-operated animals (n = 12–13, white boxes) and in the different sepsis groups representing different stages of sepsis (grey boxes). The number of animals used in various sepsis groups is indicated in Table 1. Plots demonstrate the median (horizontal line in the box) and the 25th (lower whisker) and 75th (upper whisker) percentiles. Comparison between groups was conducted with the Kruskal–Wallis test followed by Dunn's post-hoc test. $^{X}P < 0.05$ vs sham-operated groups; $^{*}P < 0.05$ vs 12 h sepsis (between sepsis groups); $^{\#}P < 0.05$ vs 24 h sepsis (between sepsis groups).

mortality was attributable to injection with *E. coli* monomicrobial cultures (Table 1). In the sepsis-inducing inocula, three bacterial phyla, including 18 mostly Gram-negative genera, could be detected. Specifically, the majority of taxa belonged to Proteobacteria (49%; e.g. *E. coli*), and the rest were distributed amongst Firmicutes (38%; e.g. Lactobacilli) and Actinobacteria (13%; e.g. *Propionibacterium acnes*) (Supplementary Table S1). The most frequent strains in the inducer inoculum were *E. coli* (in 100% of the samples), followed by *Klebsiella pneumoniae*, Pseudomonas, Bifidobacteria and Lactobacilli.

In the ascites, bacterium concentration decreased by one order of magnitude ($P < 0.01$) (Fig. 5), which was also accompanied by reduced diversity of bacterial strains during the sepsis progression (Table 1). In addition, new species also reached the detection level (Supplementary Table S1). After 72 h of sepsis, only *E. coli* (in 100% of the samples) and *Lactobacillus murinus* (in 17% of the samples) were identified in the ascites.

Association between bacterial dose of the inducer inoculum and the severity of organ failure. We also wanted to examine the influence of inoculum CFUs on organ dysfunction (as evidenced by the cumulative ROFA score). The initial CFU and ROFA scores showed a moderate relationship at 12 h (Fig. 6a). However, a significant correlation between these parameters was observed at 24 h of fecal peritonitis (Fig. 6b). No connection between the amount of injected CFU and ROFA score was evidenced at 48 and 72 h (Fig. 6c,d).

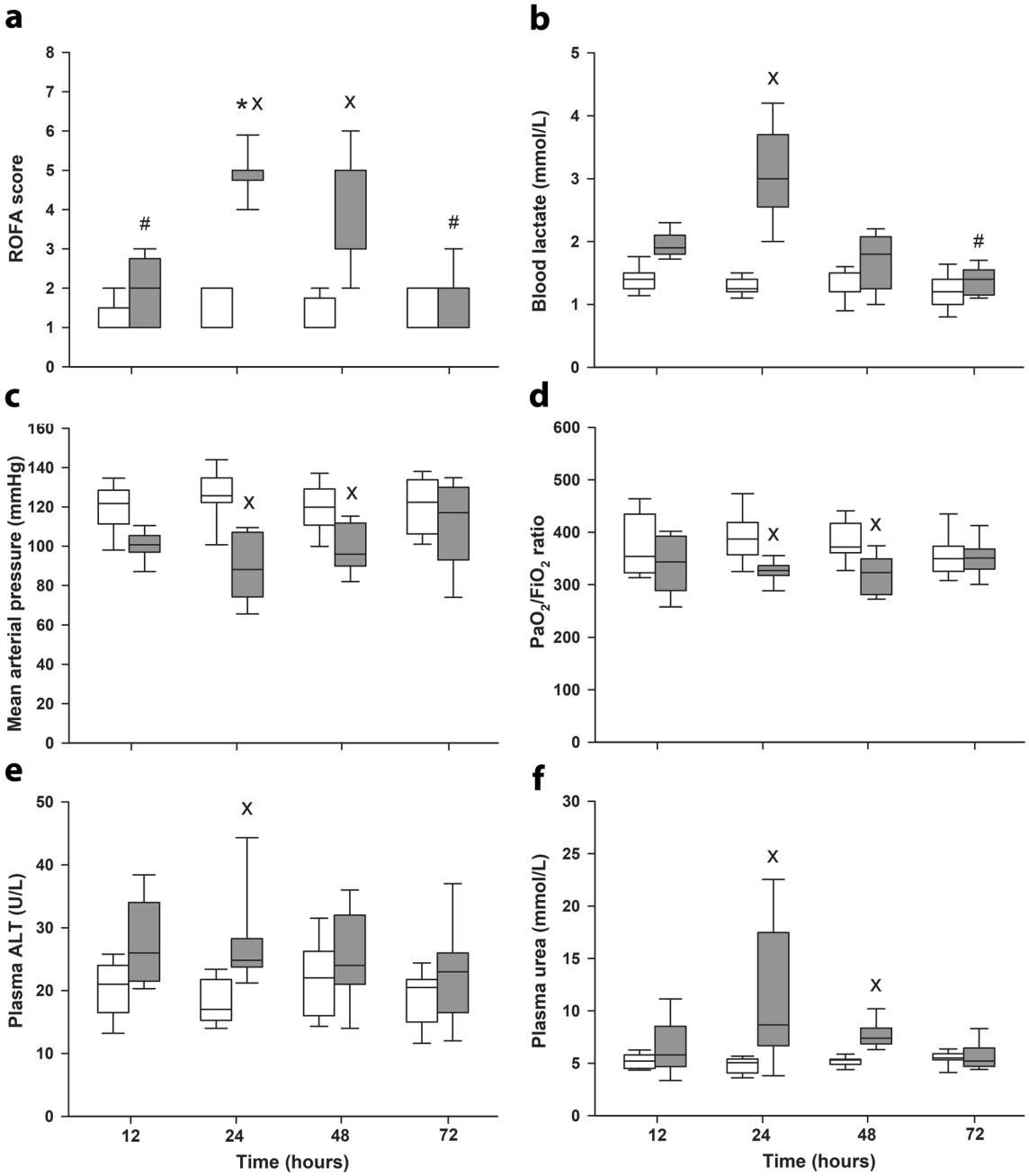

Figure 4. Rat-specific organ failure assessment (ROFA) score and its components in sham-operated animals (n = 12–13, white boxes) and in the different sepsis groups representing different stages of sepsis (grey boxes). Cumulative ROFA score (**a**), plasma lactate levels (**b**), mean arterial pressure (**c**), lung injury (represented by the Carrico index) (**d**), plasma alanine aminotransferase (ALT) (**e**) and plasma urea levels (**f**) are shown. The number of animals used in the various sepsis groups is indicated in Table 1. Comparisons between groups were conducted with the Kruskal–Wallis test followed by Dunn's post-hoc test. $^{X}P < 0.05$ vs sham-operated groups; $^{*}P < 0.05$ vs 12 h sepsis (between sepsis groups); $^{\#}P < 0.05$ vs 24 h sepsis (between sepsis groups).

ROFA score components at 24 h after mono- and polymicrobial-type inocula. Since retrospective qualitative microbiological analysis revealed marked differences in the diversity of bacterial strains (also with respect to mono- vs polymicrobial features) in the inoculum, we ran a retrospective subgroup analysis to compare the parameters of ROFA scores for animals that were found to be originally challenged with polymicrobial inoculum (in the 24-h sepsis group; n = 10) and with *E. coli* monomicrobial content in the 24, 48 and 72 h sepsis groups (n = 3, 4 and 3 animals, respectively; $n_{\Sigma} = 10$). We found significantly higher ALT and ROFA score values in animals injected with *E. coli* monomicrobial inoculum compared to the other cohort (Fig. 7a–c).

Bearing in mind the negligible quantitative differences in inocula, but the remarkably large differences in their microbiological diversity, we also retrospectively assessed how simultaneous consideration of these features influenced organ dysfunction at 24 h of sepsis. According to results from the subgroup analysis, the relationship

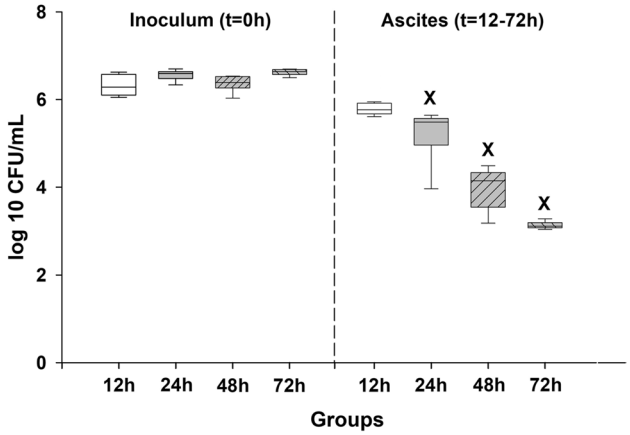

Figure 5. Bacterium concentration in the induction inocula and the abdominal fluids in the different sepsis groups representing different stages of sepsis. The number of animals used in the various sepsis groups is indicated in Table 1. Plots demonstrate the median (horizontal line in the box) and the 25th (lower whisker) and 75th (upper whisker) percentiles. Data were analyzed with two-way analysis of variance (ANOVA) followed by the Holm–Sidak post-hoc test. $^{X}P < 0.05$ vs corresponding inducer inoculum.

Groups	Type of sample	Total number of species (bacterial diversity)	Total number of animals available for sampling	Number of animals with polymicrobial culture present (mortality at 24 h)	Number of animals with *E. coli* monomicrobial culture present (mortality at 24 h)
Gr. 12 h	Inoculum	22	13	12 (0/12)	1 (0/1)
	Ascites	13	13	12	1
Gr. 24 h	Inoculum	19	13	10 (0/10)	3 (3/3)
	Ascites	9	10	6	4
Gr. 48 h	Inoculum	22	13	9 (0/9)	4 (4/4)
	Ascites	5	9	5	4
Gr. 72 h	Inoculum	21	12	9 (0/9)	3 (3/3)
	Ascites	2	9	1	8

Table 1. Bacterial diversity and sepsis-related mortality. Bacterial diversity is represented by the total number of bacterial species present in the inoculum and ascites samples in the different sepsis groups (Grs. 12–72 h). Mortality data (ratio of the numbers of animals which had to be humanely euthanized at 24 h after sepsis induction compared to the total number of animals in the given group) are indicated in brackets in the lines for the corresponding inocula.

between CFU values and ROFA scores showed a similar correlation in both the *E. coli* monomicrobial and the polymicrobial subgroups, but the slope of the regression line of the monomicrobial subgroup was greater than that of the polymicrobial subgroup (Fig. 8a).

Furthermore, the ROFA score also displayed a correlation with ascites CFU values. A significant non-linear relationship was identified between the ascites CFU and the ROFA score (3rd order polynomial regression) in polymicrobial ($P = 0.002$) or monomicrobial ($P = 0.02$) subgroups during the 12–72 h sepsis period with a shifting of the bacterial composition towards *E. coli* dominance over time (Fig. 8b).

Discussion

Our aim was to investigate the microbiological characteristics of a typical rodent model of intra-abdominal sepsis. Except for antibiotics, the study followed the recommendations in the MQTiPSS guidelines; analgesia, standard fluid therapy and strictly defined scoring systems were used to determine the progression of events[2]. The inflammatory immune response was manifested in distinctive, time-dependent increases in plasma IL-6[12] and ET-1[13] levels, and the numerical parameters of cardiovascular, pulmonary, kidney and liver functions—all included in the human SOFA scoring system—established the onset, peak and resolution. The functional changes of organ systems were accompanied by signs of subcellular metabolic dysfunction, increased blood lactate levels and reduced Complex II-linked capacity of oxidative phosphorylation of liver mitochondria. In this experimental system, the relationship between the quantified responses and the matching microbiological profile was determined sequentially, starting from the fecal induction to 72 h samples from the abdominal cavity.

A number of preclinical animal models of human sepsis with various advantages and disadvantages have already been presented to the scientific community. In general terms, CLP is considered the most effective investigative tool; nevertheless, precise control of intestinal leakage is usually impossible. Fecal inductions with

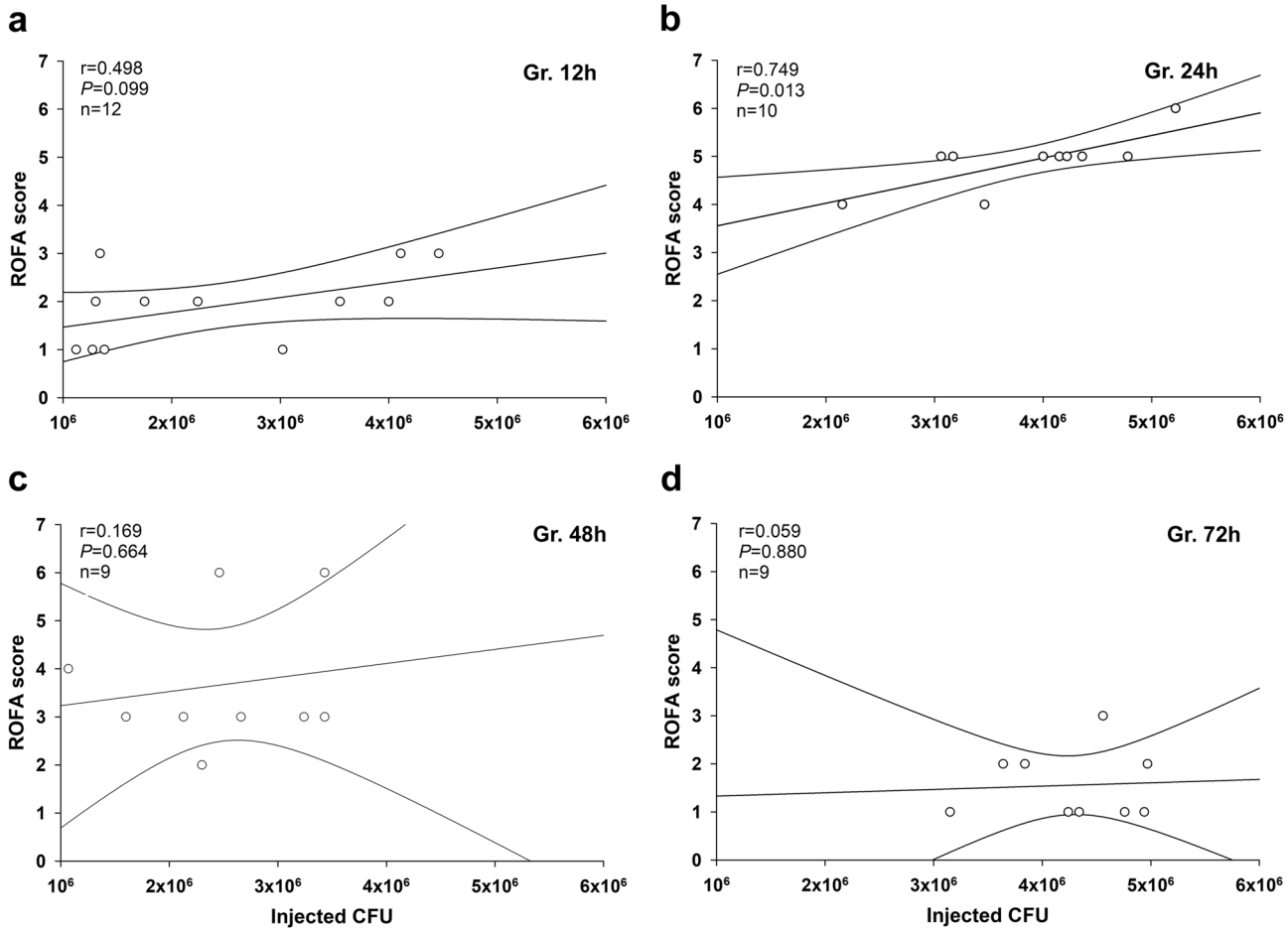

Figure 6. Correlation between CFU values of the inducer inoculum and ROFA scores. Values are shown in the 12 h **(a)**, 24 h **(b)**, 48 h **(c)** and 72 h **(d)** polymicrobial sepsis groups. The number of animals used in the various sepsis groups is indicated in Table 1. Pearson's product correlation coefficient r values and (null hypothesis-related) *P* values are provided, and regression lines and 95% confidence intervals are indicated.

standardized CFU concentration ranges are considered appropriate alternatives[14], and the bacterial load can be quantitatively defined. In our hands, 1.02×10^6–5.6×10^6 CFUs correlated well with the onset time of severe reactions 24 h later. This CFU range resulted in approx. 20% summed mortality, broadly reproducing the 17–29% mortality rate of human intra-abdominal sepsis[15]. Here it should be noted that 24 h for rats corresponds to a time interval of approx. 21 days in humans, due to the often overlooked 1:21 conversion ratio of the rat-human age correlation[16]. The changes in signs and symptoms were followed further up to 72 h; visible and measurable parameters were monitored and recorded sequentially, corresponding again to clinical practice. This approach demonstrated the resolution phase; the compensatory mechanisms led to recovery in the surviving cohort of animals between 24 and 72 h.

It should be noted that the flora of fecal peritonitis is generally considered polymicrobial, but identification of endogenous or exogenous microbial sources is usually lacking in the design of animal model strategies. *E. coli* showed the highest frequency among the sepsis-causing bacteria we isolated (followed by *Klebsiella*, *Pseudomonas* and *Acinetobacter*), which is consistent with clinical experience[17–19]. However, sepsis with a Gram-positive source in rodents is relatively rare, in contrast to the frequent occurrence of *Staphylococcus aureus* in human sepsis[19].

Due to the time burden and fastidious identification of fecal pathogens, there are likewise no established qualitative criteria in CFU values either. Here we have demonstrated the paramount importance of identifying inducer strains because approx. 20% of the fecal solutions with a presumed polymicrobial habitat proved to be monomicrobial (with only *E. coli* present). Moreover, the monomicrobial induction was attributed exclusively to the 24 h mortality, and the general condition of the hosts was more severely impaired in these cases. This finding supports the view that *E. coli* may be responsible for early mortality in intra-abdominal sepsis[20] but partially contradicts other results, where polymicrobial infections had a higher mortality rate[21].

Here it should be underlined that a shift from polymicrobial to monomicrobial content had begun during the preparation of the uniformly prepared and mixed stool samples, and the transition was then tracked in the animals' bodies. Another distinctive feature of the process was the Lactobacillus and Bifidobacteria cultures detected in the ascites perhaps as a compensatory sign of the host's bacterial defense mechanism[22]. These processes may also explain the absence of mortality in the polymicrobial sepsis group in our experiments.

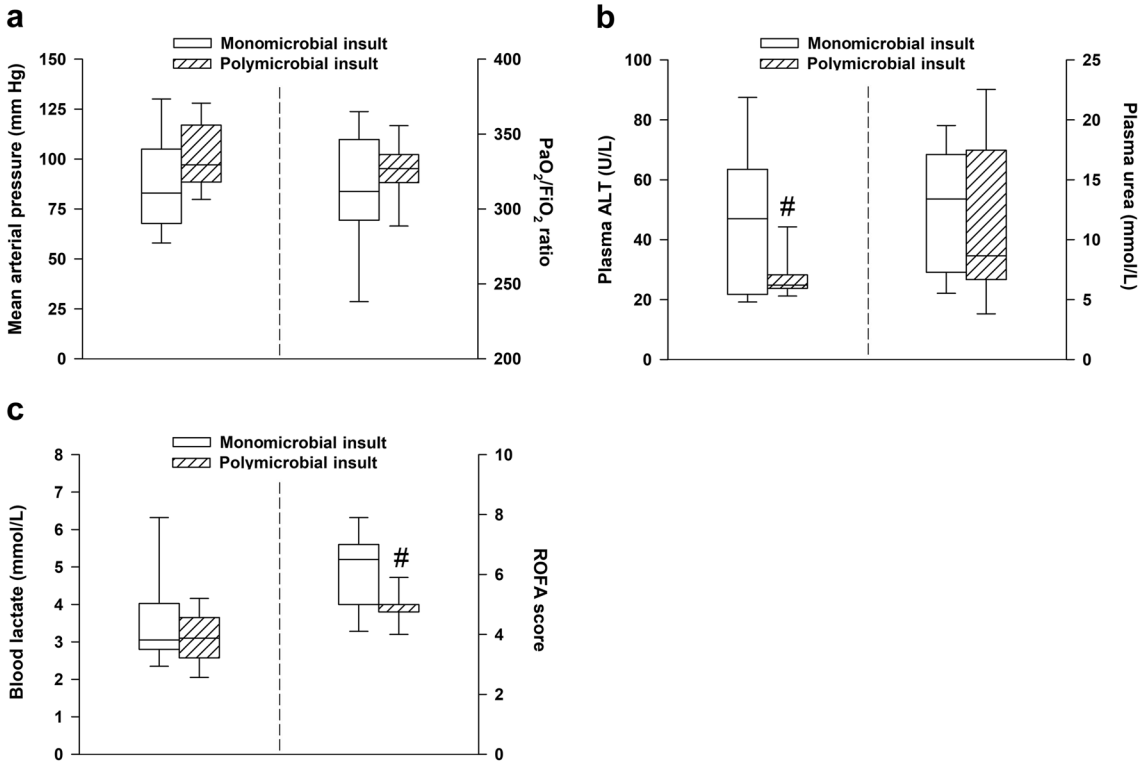

Figure 7. Comparison of rat-specific organ failure assessment (ROFA) parameters in *E. coli* monomicrobial (n = 10) or polymicrobial subgroups (n = 10) at 24 h. **(a)** Mean arterial pressure and lung injury (represented as the Carrico index), **(b)** plasma alanine aminotransferase (ALT) and plasma urea levels, **(c)** blood lactate levels and cumulative ROFA score. Plots demonstrate the median (horizontal line in the box) and the 25th (lower whisker) and 75th (upper whisker) percentiles. Between groups, comparison of ROFA score values was made with the Mann–Whitney U test, whereas ROFA components were compared with the Welch independent samples t-test. $^{\#}P < 0.05$ monomicrobial vs polymicrobial septic subgroups.

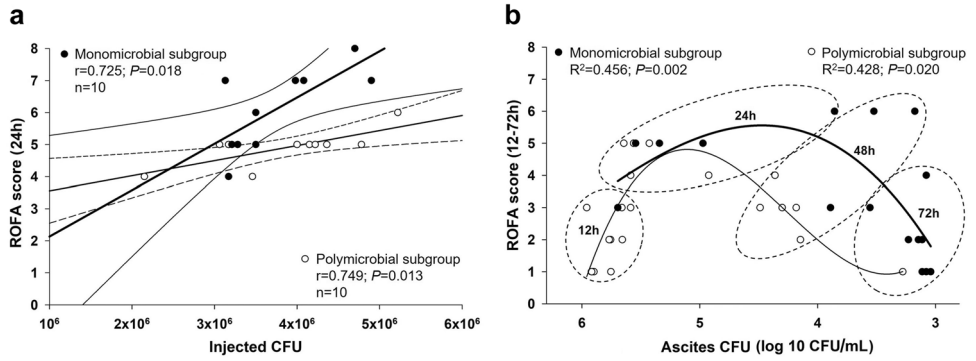

Figure 8. Correlations between inoculum and ascites CFU and ROFA score values in mono- or polymicrobial subgroups. **(a)** Correlations between CFU values for the mono- or polymicrobial inducer inoculum and ROFA scores at 24 h of sepsis. The *E. coli* monomicrobial subgroup (n = 10) is marked with black circles, a thick regression line and a thin line for the 95% confidence interval, whereas the polymicrobial subgroup (n = 10) is indicated with open circles, a thin regression line and a dashed line for the 95% confidence interval. Pearson's product correlation coefficient r values, (null hypothesis-related) *P* values and numbers of animals involved in the subgroup analysis are provided. **(b)** Relationship between the log 10 CFU values for ascites and ROFA score values in all septic groups. The number of animals in the various sepsis groups is indicated in Table 1. Evolving predominance of ascites monomicrobial (black circles) vs polymicrobial (open circles) content and reduced CFUs in ascites over time. Polynomial regression curves of the polymicrobial and monomicrobial ascites samples are marked with a thin and a thick line, respectively. Third-order polynomial curve fit values (R^2 and *P*) are indicated. Data belonging to different stages of sepsis are illustrated with dashed ellipses.

We followed the dynamics of the transition of bacterial strains in the surviving animals, and the concentration and diversity of the polymicrobial cultures in the ascites decreased after 24 h and the most frequent strain was again *E. coli*[23–25]. However, new strains (e.g. *Neissera subflavia*) were also detected over time, consistent with the number of bacteria in secondary peritonitis. Finally, the majority of the strains disappeared from the ascites, and only *E. coli* and *Lactobacillus murinus* were detected with reduced concentrations in the 72 h samples. Again, these findings indirectly support the hypothesis that Lactobacilli suppress the growth of opportunistic pathogens colonizing in the peritoneum[22].

To our knowledge, this is the first study to demonstrate the dominant appearance of *E. coli* monomicrobial cultures in association with early mortality in experimental sepsis. A natural selection that is amplified under favorable conditions is the most likely explanation for the process[26,27], leading to microbial fitness and the "survival of the meanest" phenomenon. It should be noted that the results do not contradict MQTiPSS recommendations[2], as polymicrobial induction reflects the development of human sepsis better compared to monomicrobial inoculation[14]; however, besides dose responses, there is an obvious need for additional microbial tests to identify the dynamics of microbial changes.

Limitations. Our cross-sectional characterization reflected the most important features of the clinical disease, but extended monitoring may add further information. Further, the microbial identification time can be improved with novel methods, such as broad-range PCR amplification with High-Resolution Melt Analysis[28]. Only a population of healthy animals was evaluated without age and gender differences, and a number of other variables were not collected which have been demonstrated to influence bacterial reactions, such as diet composition. It should be added that antibiotics affect mitochondrial functions and microbial reactions as well; this confounding option was therefore purposefully omitted from the protocol.

Conclusions

The colonizing bacteria in the peritoneal sac significantly influence the outcome, so strict microbiological analysis of the qualitative properties and a reliable separation of possible variations—Gram-negative, Gram-positive, mono- or polymicrobial induction types—must be controlled to properly model bacterial sepsis. A similar phenomenon may conceivably occur in human conditions, but we did not want to make assumptions. Nevertheless, enhanced understanding of the relative emergence of dominant strains or species in a mixed culture and the competitive intraperitoneal bacterial responses is likely to improve translational research success. Qualitative microbial changes are of pivotal impact in the pathophysiology, the unknown microbiological profile may define/restrict the usability of rodent sepsis models.

Materials and methods

Animals. Male Sprague–Dawley rats (380 ± 30 g bw) were used with adherence to NIH guidelines and EU directive 2010/63/EU for the protection of animals used for scientific purposes, and the study was approved by the national competent authority of Hungary (ATET; V/175/2018). The animals were housed in plastic cages (21–23 ℃) with a 12/12 h dark–light cycle and access to standard rodent food and water ad libitum. The study design and the presentation of the data are in accordance with the MQTiPSS recommendations and with the Animal Research: Reporting of In Vivo Experiments guidelines (https://arriveguidelines.org/).

Preparation of the sepsis-inducing fecal inoculum. Our aim was to induce peritoneal sepsis with injections of standardized bacterial counts within a defined range, but without limiting the variability in the microbiome composition. Therefore, we did not use a single stock of feces; instead, we prepared fresh fecal inocula on a daily basis (using a standardized method, see below) and injected a maximum of four rats per day according to a predefined randomization protocol (Fig. 1a). This protocol was repeated several times consecutively throughout the duration of the study.

Fresh feces (~ 4 g) was randomly collected from age and body weight-matched healthy rats (n = 4–5) 18 h before the scheduled intra-abdominal injections. The fecal mass was mixed with 6 mL saline in sterile 10 mL Falcon tubes, vortexed and incubated for 6 h at 37 ℃. After a 3:1 dilution, the suspension was filtered to remove the pellet. For microbiological analysis, 0.1 mL samples were taken from the suspension to determine the number of CFUs and identify the strains (qualitative analyses; see later), and the rest of the filtrate was stored at 4 ℃ for 12 h (the typical time required to determine CFUs). In prior studies, we proved that a 6-h incubation period and a 12-h cold storage had no significant effect on the quantitative and qualitative characteristics of these fecal suspensions (Supplementary Fig. S1, Supplementary Table S2).

Sepsis induction, and experimental setup and groups. The optimal germ count required for reproducible sepsis induction (the relationship between CFUs and mortality rate) was determined in another 24 h pilot study (n = 12, Supplementary Material S1). Based on these in vivo data, the filtered inoculum was injected intraperitoneally (ip.) using a 21G needle in a volume of 5 mL/kg at a dose range of 1.02×10^6–5.6×10^6 CFU. Rats in the sham-operated groups received saline in the same volume. Sample size estimation was performed assuming approx. 20% mortality after 24 h. If the presumed true hazard ratio of septic subjects relative to controls is 0.2 with a power of $1 - \beta = 0.9$ and the Type I error probability is $\alpha = 0.05$, the inclusion of 12 septic and 12 control animals was recommended in each selected time point. In line with the sample size estimation, the animals were randomly assigned to sham-operated ($n_{\Sigma} = 49$) and septic groups ($n_{\Sigma} = 51$), which were randomly further divided into four independent groups each (sham-operated: $n_{12h} = 13$, $n_{24h} = 12$, $n_{48h} = 12$, $n_{72h} = 12$; septic: $n_{12h} = 13$, $n_{24h} = 13$, $n_{48h} = 13$, $n_{72h} = 12$) according to a termination timeline set between 12 and 72 h (Fig. 1a).

ROFA score	Plasma lactate (mmol/L)	MAP (mm Hg)	PaO_2/FiO_2 ratio	Plasma ALT (U/L)	Plasma urea (mmol/L)
0	< 1.64	> 75	> 400	< 17.5	< 7.5
1	1.64 < 3	65 < 75	300 < 400	17.5–30.2	7.5–21
2	3 < 4	55 < 65	200 < 300	> 30.2	> 21
3	4 < 5	< 55	100 < 200	–	–
4	> 5	–	< 100	–	–

Table 2. Threshold values of the components of rat-specific organ failure assessment (ROFA) scoring system. Sepsis was defined as cumulative ROFA score above 2. *MAP* mean arterial pressure, *ALT* alanine aminotransferase.

Assessments and measurements. *Quantitative microbiological analysis.* The number of CFUs was determined with the standard pour-plate count method[29] and converted to the cell number per milliliter of the original inocula (CFU/mL). Briefly, a 0.1 mL sample of the final suspension was diluted (1:10), and the dilutions were spread with a glass rod on solid media (Tryptic Soy Agar; Merck, Darmstadt, Germany) under sterile conditions, incubated for 12 h at 37 ℃. Thereafter, the bacterium concentration was assessed by averaging the counted colonies multiplied by the appropriate dilution factor.

Qualitative microbiological analysis. The bacterial composition of the inoculum was analyzed with species-selective media for the most frequent species and by MALDI-TOF mass spectrometry (MS; Bruker Daltonics, Germany). A 0.1 mL of the suspension was spread on Mueller–Hinton solid media (Bio-Rad, Budapest, Hungary) to identify the aerobe strains. After a 12 h incubation period at 37 °C, colonies from the mixed culture were isolated to form pure bacterium cultures. Anaerobe strains were inoculated on Columbia agar base (Oxoid, Budapest, Hungary) supplemented with 5% (v/v) bovine blood, hemin (1 mg/ mL) and vitamin K1 (5 mg/mL) for 48 h at 37 °C; anaerobes were incubated in an anaerobic chamber (Bactron, Sheldon Manufacturing, Cornelius, Oregon, US).

Sample preparation for MALDI-TOF MS measurement was performed as described earlier[30]. In brief, the spectra from the microbiological samples were acquired using the Microflex LT system (Bruker Daltonik, Bremen, Germany) and analyzed with MALDI BIOTYPER 3.3 (Bruker Daltonik, Bremen, Germany) software. MALDI-TOF MS analysis was performed in triplicate, with parallel tests performed on the same target plate. The mass spectrometric identification of the microorganisms was confirmed if the score for at least one of three spots was above 2.0 (species level) and above 1.7 (genus level)[31,32]. The results of the bacterium composition were always available 48 h after the end of the preparation procedure of the inoculum.

Animal well-being. The general condition of the animals was evaluated at 6 h after the ip. injections and every 12 h thereafter using a modified 0–9 point rat-specific RSS scoring system[33], where a cumulative value above 6 was considered a humane endpoint for euthanasia (Supplementary Table S3). At time points of sickness assessment, the animals received 10 mL/kg crystalloid solution sc. (Ringerfundin, B. Braun, Hungary) to avoid dehydration and 15 μg/kg buprenorphine sc. (Bupaq, Merck, USA) to maintain analgesia[2].

Hemodynamic measurements: blood and tissue sampling. At the predetermined timeline (12 h, 24 h, 48 h or 72 h after induction), the animals were anesthetized with a mixture of ketamine (45.7 mg/kg ip.) and xylazine (9.14 mg/kg ip.) and placed on a heating pad to maintain body temperature at 37 ℃. Tracheostomy was performed, with the right jugular vein cannulated for fluid infusion (10 mL/kg/h Ringerfundin) and continuous anesthesia (12.2 mg/kg ketamine, 2.52 mg/kg xylazine and 0.612 mg/kg diazepam iv.). The left carotid artery was cannulated to monitor mean arterial blood pressure and heart rate (Cardiosys 1.4, Experimetria Ltd., Budapest, Hungary). After an approx. 30-min surgical preparation and 15-min stabilization, hemodynamic monitoring was performed for 30 min. Arterial and venous blood samples were collected for blood gas (Cobas b123, Roche Ltd., Basel, Switzerland) and blood lactate analysis (Accutrend Plus, Roche, Hungary). Based on a standard formula $(SaO_2 - SvO_2)/SaO_2)$, simplified OER was calculated from arterial (SaO_2) and venous oxygen saturations (SvO_2). Lung function was determined by calculating the PaO_2/FiO_2 ratio (Carrico index) from partial arterial oxygen pressure (PaO_2) and FiO_2 (which was 0.21).

After recording for 30 min, a sterile midline laparotomy was performed and a 0.1 mL fluid sample was taken from the abdominal cavity for microbiological analysis[30]. Next, a tissue biopsy was taken from the left lateral lobe of the liver in cold phosphate-buffered saline to measure mitochondrial functions (see later), and blood samples were collected from the inferior caval vein (see later) using a sterile technique. After sampling, the rats were euthanized with an overdose of ketamine (120 mg/kg).

Sequential organ failure assessments. The severity of organ dysfunction was determined with the ROFA scoring system[2,9], which simultaneously considers not only cardiovascular, respiratory, hepatic and renal damage/dysfunction, but also blood lactate levels. Based on this scoring, sepsis was defined as a cumulative ROFA score above 2 (Table 2).

Measurements of inflammatory and organ function-related markers. Blood samples were collected from the inferior vena cava into pre-cooled, EDTA-coated tubes, centrifuged (1200×*g* at 4 °C for 10 min) and stored at − 70 °C. Plasma IL-6 and ET-1 levels were determined with standard ELISA kits (Cusabio Biotechnology Ltd., Wuhan, China, and Biomedica Ltd., Vienna, Austria, respectively). Kidney injury was determined from plasma urea level, whereas liver dysfunction was assessed by measuring the plasma alanine aminotransferase (ALT) level, using a Roche/Hitachi 917 analyzer (F. Hoffmann-La Roche AG, Switzerland). All analyses were performed on coded samples in a blinded fashion.

Examination of mitochondrial function. Mitochondrial respiration from liver homogenates was determined using high-resolution FluoRespirometry (Oxygraph-2k, Oroboros, Innsbruck, Austria) as described previously[9]. In brief, after Complex I (CI) inhibition by rotenone (0.5 µmol/L, Merck, USA), samples were stimulated with Complex II (CII)-specific substrate (succinate, 10 mM, Merck, USA) for measuring LEAK respiration ($LEAK_S$). CII-linked oxidative phosphorylation (OXPHOS CII) was determined at a saturation concentration of ADP (5 mmol/L, Merck, USA). ATP synthase was inhibited by oligomycin (2.5 µmol/L) to assess LEAK respiration in a non-phosphorylating state ($LEAK_{Omy}$). At the end of the protocol, mitochondrial respiration was blocked by Complex III inhibitor Antimycin A (2.5 µmol/L, Merck, USA) to evaluate residual oxygen consumption (ROX). Mitochondrial oxygen consumption (volume-specific flux, JO_2) was expressed in pmol/s/mL.

Statistical analysis. Data were evaluated with the SigmaStat 12.5 software package (Systat Software, San Jose, CA) or the IBM SPSS 26 software (IBM Corp., Armonk, NY). Survival was analyzed and plotted using the Kaplan–Meier method. Based on data distribution (Shapiro–Wilk test), non-parametric (Mann–Whitney, Kruskal–Wallis or Friedman analysis of variance on ranks tests with the Dunn's post-h test) or parametric methods (t-test and two-way analysis of variance followed by the Holm–Sidak test) were used. Data were displayed as median values and interquartile ranges of the 75th and 25th percentiles, with $P < 0.05$ being considered significant. The Pearson's method was used for analysis of linear correlation (correlation coefficient (r), regression lines and 95% confidence intervals were indicated), whereas the non-linear relationship was examined with the cubic polynomial regression analysis (trend line, R^2 and *P*-values were provided).

Data availability

All data generated or analyzed during this study are included in this published article (and its Supplementary Information files).

Received: 13 May 2021; Accepted: 3 November 2021
Published online: 23 November 2021

References

1. Osuchowski, M. F. *et al.* Minimum quality threshold in pre-clinical sepsis studies (MQTiPSS): An international expert consensus initiative for improvement of animal modeling in sepsis. *Shock* **50**, 377–380 (2018).
2. Vincent, J. L. *et al.* The SOFA (sepsis-related organ failure assessment) score to describe organ dysfunction/failure. *Intens. Care Med.* **22**, 707–710 (1996).
3. Singer, M. *et al.* The third international consensus definitions for sepsis and septic shock (Sepsis-3). *J. Am. Med. Assoc.* **315**, 801–810 (2016).
4. Lewis, A. J., Seymour, C. W. & Rosengart, M. R. Current murine models of sepsis. *Surg. Infect.* **17**, 385–393 (2016).
5. Deitch, E. A. Rodent models of intra-abdominal infection. *Shock* **24**, 19–23 (2005).
6. Liu, X. *et al.* Consistency and pathophysiological characterization of a rat polymicrobial sepsis model via the improved cecal ligation and puncture surgery. *Int. Immunopharmacol.* **32**, 66–75 (2016).
7. Murando, F., Peloso, A. & Cobianchi, L. Experimental abdominal sepsis: Sticking to an awkward but still useful translational model. *Mediat. Inflamm.* **6**, 1–8 (2019).
8. Nandi, M. *et al.* Rethinking animal models of sepsis—Working towards improved clinical translation whilst integrating the 3Rs. *Clin. Sci. (Lond.)* **134**, 1715–1734 (2020).
9. Juhász, L. *et al.* Divergent effects of the N-methyl-D-aspartate receptor antagonist kynurenic acid and the synthetic analog SZR-72 on microcirculatory and mitochondrial dysfunction in experimental sepsis. *Front. Med.* **7**, 848 (2020).
10. Burch, P. T., Scott, M. J., Wortz, G. N., Peyton, J. C. & Cheadle, W. G. Mortality in murine peritonitis correlates with increased *Escherichia coli* adherence to the intestinal mucosa. *Am. Surg.* **70**, 333–341 (2004).
11. Nemzek, J. A., Hugunin, K. M. S. & Opp, M. R. Modeling sepsis in the laboratory: Merging sound science with animal well-being. *Comp. Med.* **58**, 120–128 (2008).
12. Shimazui, T., Matsumura, Y., Nakada, T. & Oda, S. Serum levels of interleukin-6 may predict organ dysfunction earlier than SOFA score. *Acute Med. Surg.* **4**, 255–261 (2017).
13. Freeman, B. D., Machado, F. S., Tanowitz, H. B. & Desruisseaux, M. S. Endothelin-1 and its role in the pathogenesis of infectious diseases. *Life Sci.* **118**, 110 (2014).
14. Garrido, A. G., de Figueiredo, L. F. P. & Silva, M. R. E. Experimental models of sepsis and septic shock: An overview. *Acta Cir. Bras.* **19**, 82–88 (2004).
15. Claridge, J. A. *et al.* Bacterial species-specific hospital mortality rate for intra-abdominal infections. *Surg. Infect. (Larchmt)* **15**, 194–199 (2014).
16. Pallav, S. The Laboratory rat: Relating its age with human's. *Int. J. Prev. Med.* **4**, 624–630 (2013).
17. Dolin, H. H., Papadimos, T. J., Chen, X. & Pan, Z. K. Characterization of pathogenic sepsis etiologies and patient profiles: A novel approach to triage and treatment. *Microbiol. Insights* **12**, 1178636118825081 (2019).
18. Grondman, I., Pirvu, A., Riza, A., Ioana, M. & Netea, M. G. Biomarkers of inflammation and the etiology of sepsis. *Biochem. Soc. Trans.* **48**, 1–14 (2020).
19. Poli-de-Figueiredo, L. F., Garrido, A. G., Nakagawa, N. & Sannomiya, P. Experimental models of sepsis and their clinical relevance. *Shock* **30**, 53–59 (2008).
20. Shah, P. M. *et al.* Do polymicrobial intra-abdominal infections have worse outcomes than monomicrobial intra-abdominal infections? *Surg. Infect. (Larchmt)* **17**, 27–31 (2016).

21. Aliaga, L., Mediavilla, J. D., Llosá, J., Miranda, C. & Rosa-Fraile, M. Clinical significance of polymicrobial versus monomicrobial bacteremia involving *Pseudomonas aeruginosa*. *Eur. J. Clin. Microbiol. Infect. Dis.* **19**, 871–874 (2000).
22. Liu, D. Q., Gao, Q. Y., Liu, H. B., Li, D. H. & Wu, S. W. Probiotics improve survival of septic rats by suppressing conditioned pathogens in ascites. *World J. Gastroenterol.* **19**, 4053–4059 (2013).
23. Barrera, G. *et al.* Model of polymicrobial peritonitis that induces the proinflammatory and immunosuppressive phases of sepsis. *Infect. Immun.* **79**, 1280–1288 (2011).
24. Almeida, J., Galhenage, S., Yu, J., Kurtovic, J. & Riordan, S. M. Gut flora and bacterial translocation in chronic liver disease. *World J. Gastroenterol.* **12**, 1493 (2006).
25. Priya, S. & Blekhman, R. Population dynamics of the human gut microbiome. Change is the only constant. *Genome Biol.* **20**, 150 (2019).
26. Russo, T. A., Carlino, U. B., Mong, A. & Jodush, S. T. Identification of genes in an extraintestinal isolate of *Escherichia coli* with increased expression after exposure to human urine. *Infect. Immun.* **67**, 5306–5314 (1999).
27. Mühldorfer, I. & Hacker, J. Genetic aspects of *Escherichia coli* virulence. *Microb. Pathog.* **16**, 171–181 (1994).
28. Hjelmsø, M. H. *et al.* High-resolution melt analysis for rapid comparison of bacterial community compositions. *Appl. Environ. Microbiol.* **80**, 3568–3575 (2014).
29. Sanders, E. R. Aseptic laboratory techniques: Plating methods. *J. Vis. Exp.* **63**, 3064 (2012).
30. Nagy, E., Becker, S., Kostrzewa, M., Barta, N. & Urbán, E. The value of MALDI-TOF MS for the identification of clinically relevant anaerobic bacteria in routine laboratories. *J. Med. Microbiol.* **61**, 1393–1400 (2012).
31. Sauer, S. *et al.* Classification and identification of bacteria by mass spectrometry and computational analysis. *PLoS ONE* **3**, e2843 (2008).
32. Idelevich, E. A. *et al.* Rapid identification of microorganisms from positive blood cultures by MALDI-TOF mass spectrometry subsequent to very short-term incubation on solid medium. *Clin. Microbiol. Infect.* **20**, 1001–1006 (2014).
33. Rademann, P. *et al.* Mitochondria-targeted antioxidants SkQ1 and MitoTEMPO failed to exert a long-term beneficial effect in murine polymicrobial sepsis. *Oxid. Med. Cell. Longev.* **2017**, 6412682 (2017).

Acknowledgements

JK was supported by NKFIH K116689 and GINOP-2.3.2-15-2016-00034 Grants. This research was conducted with the support of the University of Szeged Open Access Fund (Grant Number: 5340), and of the Szeged Scientists Academy under the sponsorship of the Hungarian Ministry of Human Capacities (EMMI:13725-2/2018/INTFIN).

Author contributions

S.P.T., M.Z.P., A.R. and R.F. performed the in vivo experiments. L.J. and M.Z.P. carried out the biochemical measurements. S.P.T., J.S. and K.B. conducted the microbiological analysis. S.P.T., M.Z.P., J.K., A.S. and M.B. wrote the manuscript. S.P.T., M.Z.P. and A.S. prepared the figures. A.S., J.K. and M.B. supervised and edited the manuscript. All authors read and approved the manuscript.

Competing interests

The authors declare no competing interests.

Additional information

Supplementary Information The online version contains supplementary material available at https://doi.org/10.1038/s41598-021-02129-x.

Correspondence and requests for materials should be addressed to J.K.

Reprints and permissions information is available at www.nature.com/reprints.

Publisher's note Springer Nature remains neutral with regard to jurisdictional claims in published maps and institutional affiliations.

Paper II

scientific reports

Check for updates

OPEN

Microcirculation-driven mitochondrion dysfunction during the progression of experimental sepsis

Roland Fejes[1], Attila Rutai[1], László Juhász[1], Marietta Zita Poles[1], Andrea Szabó[1], József Kaszaki[1], Mihály Boros[1,2]✉ & Szabolcs Péter Tallósy[1,2]✉

Sepsis is accompanied by a less-known mismatch between hemodynamics and mitochondrial respiration. We aimed to characterize the relationship and time dependency of microcirculatory and mitochondrial functions in a rodent model of intraabdominal sepsis. Fecal peritonitis was induced in rats, and multi-organ failure (MOF) was evaluated 12, 16, 20, 24 or 28 h later (n = 8/group, each) using rat-specific organ failure assessment (ROFA) scores. Ileal microcirculation (proportion of perfused microvessels (PPV), microvascular flow index (MFI) and heterogeneity index (HI)) was monitored by intravital video microscopy, and mitochondrial respiration (OxPhos) and outer membrane (mtOM) damage were measured with high-resolution respirometry. MOF progression was evidenced by increased ROFA scores; microcirculatory parameters followed a parallel time course from the 16th to 28th h. Mitochondrial dysfunction commenced with a 4-h time lag with signs of mtOM damage, which correlated significantly with PPV, while no correlation was found between HI and OxPhos. High diagnostic value was demonstrated for PPV, mtOM damage and lactate levels for predicting MOF. Our findings indicate insufficient splanchnic microcirculation to be a possible predictor for MOF that develops before the start of mitochondrial dysfunction. The adequate subcellular compensatory capacity suggests the presence of mitochondrial subpopulations with differing sensitivity to septic insults.

The progression of sepsis is accompanied by an imbalance between oxygen delivery (DO_2) and consumption (VO_2), and the associated microcirculatory-mitochondrial dysfunction syndrome (MMDS) is generally considered to be the driver of multi-organ failure (MOF)[1,2]. The advancing feature of this process implies ongoing changes or amplifying loops which may involve the main MMDS components towards organ malfunction to different degrees[3–7]. Nevertheless, the onset of MOF is a definite turning point in the trajectory of events, since "before and after MOF" periods have different impacts on the outcome[8]. Certainly, this issue is of critical importance as clinical diagnostics and therapeutic decisions can all be tailored or fine-tuned to the complementary parts of a progressive syndrome.

It should be noted here that systemic hemodynamics and global oxygenation parameters usually do not follow the progression tightly, and microcirculatory oxygen transport in this scheme seems relatively independent of macrohemodynamic variables[9,10]. Similarly, it has been proposed that microcirculatory status is a better predictor not only of the severity of MOF but also of sepsis mortality. Indeed, algorithms that support microcirculatory DO_2 for an upkept mitochondrial VO_2 are in the focus of clinical and basic research interest[11].

It should also be added that increased cardiac output and higher metabolic rate with preserved capillary perfusion in vital organs usually prevail during the acute hyperdynamic phase of sepsis[12–15]. The early mitochondrial reaction is largely tissue-dependent, but in most cases, it is characterized by increased VO_2 and a shift to a catabolic state. Thereafter, a plateau is reached and the hypodynamic phase involves reduced cardiac performance, tissue hypoperfusion with hyperlacticemia and other signs of mitochondrial and organ damage[16,17]. In this simplified outline, tissue mitochondria together with their supplier microcirculatory network are both significant driving forces for the development of MOF. However, it remains an open question whether these

[1]Institute of Surgical Research, Albert Szent-Györgyi Medical School, University of Szeged, Szeged 6720, Hungary. [2]These authors contributed equally: Mihály Boros and Szabolcs Péter Tallósy. ✉email: boros.mihaly@med.u-szeged.hu; tallosy.szabolcs@med.u-szeged.hu

changes are causally related and, if so, how this bidirectional connection develops in time. Indeed, there are three possibilities for mitochondrial dysfunction: it may be a direct and early consequence of microcirculatory failure, thus being the promoter of progression; it can occur in parallel with microcirculatory events, interacting continuously in a vicious circle and influencing the outcome jointly; or, theoretically, it can occur independently of microcirculatory impairment.

It is challenging to demonstrate causal links between the microcirculatory and mitochondrial arms of MMDS even in standardized experimental conditions due to the web of connections and cross-reactions which make it difficult to interpret findings accurately. Of note, the microcirculatory and mitochondrial changes have not been investigated simultaneously in human sepsis in the pre- and post-MOF periods[18–20]. We have therefore designed an in vivo study to monitor the splanchnic microvascular status and the concurrent mitochondrial function simultaneously, together with other signs of the septic response in an accepted preclinical model of intraabdominal sepsis. In this longitudinal protocol the animals were randomly allocated into independent groups during different periods (from 12 to 28 h) of sepsis progression. This protocol allowed us to investigate the correlation between established variables of microcirculatory or mitochondrial dysfunction and to determine their predictive diagnostic value in the course of experimental sepsis.

Results

Animal well-being and time-dependent changes in multi-organ failure markers

Assessments of animal well-being and organ dysfunction were performed using RSS scores (rat-specific, well-being-related sickness score) and the ROFA scoring (rat-specific organ failure assessment) system, respectively, while the termination of experiments was scheduled at predetermined time points (12th h, 16th h, 20th h, 24th h and 28th h) after sepsis induction (Fig. 1a). There were no significant changes in the RSS score in the sham-operated group. Septic groups between the 20th and 24th h elevated significantly not only compared to the 12th h septic sham-operated group but also compared to the 20th and 24th h sham-operated groups (see Supplementary Fig. S1 online). Three animals were euthanized (one at the 20th h and two more at the 24th h) due to the critically elevated RSS score (at least 6 points). The number of euthanized animals is included in the mortality calculations (Fig. 1b). IL-6 significantly increased as compared to the control group, peaking at the 16th h ($P < 0.001$), after which a decrease started reaching the level of the sham-operated group after the 24th h (Table 1). ROFA parameters were significantly higher in the septic groups compared to the sham-operated animals during the whole experimental period, with the score reaching its maximum at the 20th h ($P = 0.007$; Table 1).

Time-dependent changes in macrohemodynamics

The changes in macrohemodynamic parameters are demonstrated in Table 1. In the sham-operated group, there were no significant hemodynamic changes over time. Sepsis was characterized by significant hypotension between the 16th and 24th h ($P_{16h} = 0.05$; $P_{20h} < 0.001$; $P_{24h} = 0.001$) compared to the sham-operated animals in the same time points. An increasing trend was observed in CO data until the 16th h ($P < 0.001$), and then CO dropped significantly below the level of the sham-operated animals at the 20th h ($P < 0.001$). Later, CO values did not differ from the controls. In the 16–24 h interval, the CO values differed significantly from the values of the 12th h group, albeit in a different way ($P_{16h} = 0.009$; $P_{20h} < 0.001$; $P_{24h} = 0.008$).

Time-dependent changes in oxygen dynamics

The numerical parameters of oxygen dynamics are indicated in Table 1. DO_2 showed a progressive decline in the septic group, reaching its lowest value at the 20th h, thereafter exceeding the levels for sham-operated animals at the 28th h. There was no significant change in VO_2 except at the 16th h ($P = 0.008$). ExO_2 rose until the 20th h when the trend reversed and did not alter from the values of the sham-operated groups. In the 16th–24th h

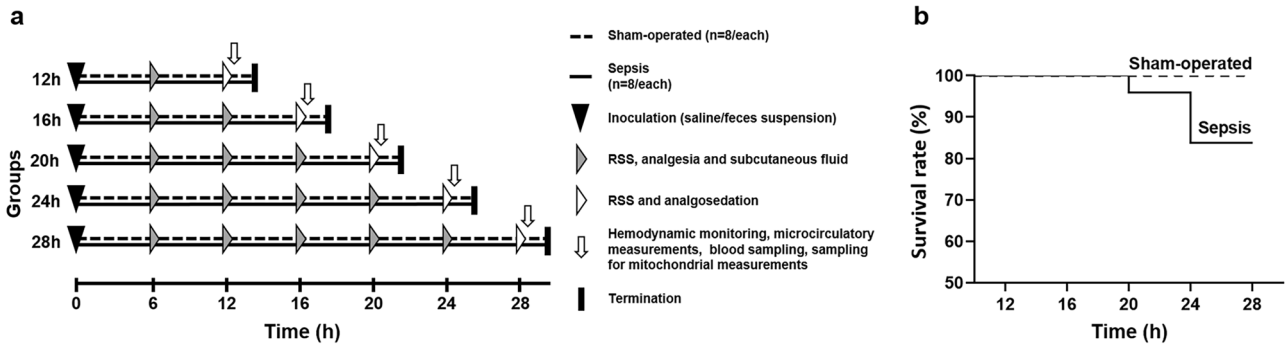

Figure 1. The experimental protocol and mortality during the study. The experimental protocol (**a**) shows groups, interventions and assessments. The animals were randomly assigned to sham-operated and septic groups, which were further divided into five subgroups each according to the length of sepsis progression (12th, 16th, 20th, 24th and 28th h). Interventions and assessments are marked with symbols. Kaplan–Meier analysis (**b**) was performed to describe survival of experimental animals. One animal in the 20th h septic and two animals in the 24th h septic group were sacrificed due to the critical level of suffering caused by sepsis induction.

Parameters	Groups	Time (h)				
		12	16	20	24	28
Cardiac output (mL/min/kg)	Sham-operated	132.00 (119.75; 140.50)	124.00 (112.25; 132.50)	125.00 (118.00; 134.25)	121.50 (116.00; 131.50)	129.50 (113.75; 138.25)
	Septic	136.50 (133.25; 151.75)	**155.00 (148.25; 171.00)**^{*x}	**96.00 (87.00; 108.00)**^{*x}	**120.50 (117.00; 126.50)**^{x}	131.50 (116.00; 139.50)
Mean arterial pressure (mm Hg)	Sham-operated	110.00 (99.75; 123.00)	105.50 (102.00; 125.75)	108.00 (99.75; 119.25)	108.00 (103.50; 115.75)	101.00 (97.50; 105.50)
	Septic	100.50 (93.75; 104.50)	**100.50 (89.50; 105.00)***	**82.00 (70.00; 92.00)**^{*x}	**88.00 (69.25; 97.25)***	112.50 (97.75; 133.25)
Oxygen extraction (%)	Sham-operated	21.77 (18.31; 33.52)	12.12 (9.47; 19.71)	30.89 (23.34; 41.56)	17.77 (11.35; 25.53)	15.54 (12.03; 19.98)
	Septic	**8.62 (7.22; 11.51)***	**33.31 (13.88; 45.02)**^{*x}	**37.01 (15.21; 50.52)**^{x}	**23.66 (14.66; 47.39)**^{x}	13.72 (11.14; 31.61)
Oxygen delivery (mL/min/1,000)	Sham-operated	66.48 (57.87; 81.11)	63.31 (52.45; 79.06)	64.82 (57.39; 71.51)	63.93 (55.86; 70.82)	65.10 (59.13; 75.59)
	Septic	**105.12 (91.22; 110.67)***	**80.21 (65.65; 85.27)**^{x}	**46.135 (37.54; 55.02)**^{*x}	**54.40 (37.95; 61.37)**^{x}	**88.57 (73.17; 98.35)***
Oxygen consumption (mL/min/1,000)	Sham-operated	13.97 (12.86; 22.52)	7.56 (5.67; 18.65)	20.13 (16.04; 27.75)	10.15 (8.42; 17.16)	9.85 (7.84; 12.15)
	Septic	9.34 (6.84; 15.64)	**27.22 (11.36; 29.54)**^{*x}	16.42 (6.34; 28.68)	12.80 (6.254; 22.523)	12.15 (10.89; 23.80)
Plasma IL-6 (pg/mL)	Sham-operated	8.2 (1.64; 13.74)	3.18 (0.72; 12.25)	8.62 (1.76; 17.65)	18.85 (10.03; 32.25)	3.18 (0.650; 9.09)
	Septic	**18.45 (13.85; 51.03)***	**52.25 (13.53; 95.33)***	**49.00 (18.70; 68.00)***	16.05 (11.70; 39.88)	**40.85 (5.68; 62.60)***
Whole blood lactate (mmol/L)	Sham-operated	0.90 (0.90; 0.90)	0.00 (0.00; 0.00)	0.90 (0.90; 0.90)	1.20 (0.00; 1.58)	0.85 (0.45; 1.33)
	Septic	1.55 (1.38; 1.95)	**3.25 (2.14; 3.83)***	3.60 (2.25; 4.65)	2.75 (2.48; 2.95)	1.60 (0.80; 2.25)
PaO_2/FiO_2 ratio	Sham-operated	406.95 (402.45; 420.88)	401.00 (383.10; 402.45)	355.71 (338.93; 369.41)	395.62 (357.98; 401.25)	373.83 (332.26; 405.81)
	Septic	363.14 (332.14; 383.45)	**292.33 (277.62; 327.80)***	348.00 (305.17; 374.76)	291.19 (221.99; 311.07)	364.05 (322.26; 375.24)
Plasma ALT (U/L)	Sham-operated	33.00 (30.13; 35.25)	44.00 (39.00; 47.75)	41.50 (35.75; 45.50)	41.00 (31.00; 51.00)	37.00 (46.75; 42.25)
	Septic	40.50 (36.50; 49.50)	35.50 (33.00; 70.50)	**24.00 (22.25; 25.00)**^{x}	31.00 (26.00; 32.50)	51.50 (42.25; 60.75)
Plasma AST (U/L)	Sham-operated	44.17 (40.74; 52.15)	65.52 (59.19; 85.05)	71.57 (54.74; 93.06)	73.80 (54.77; 90.95)	48.77 (37.49; 79.94)
	Septic	**92.55 (71.43; 118.73)***	145.20 (91.65; 176. 91)	44.69 (36.55; 72.44)	50.40 (42.30; 78.09)	90.14 (60.88; 115.41)
Plasma urea (mmol/L)	Sham-operated	5.55 (4.38; 6.85)	4.95 (4.55; 6.55)	5.10 (4.38; 5.88)	4.90 (4.23; 6.90)	6.45 (5.10; 7.28)
	Septic	9.55 (5.60; 11.83)	7.75 (5.85; 10.90)	7.60 (6.30; 20.10)	8.25 (6.63; 9.20)	6.30 (5.43; 8.70)
ROFA score	Sham-operated	0.50 (0.00; 1.00)	1.00 (0.00; 1.00)	1.00 (0.25; 2.00)	1.00 (1.00; 2.00)	1.00 (0.25; 1.38)
	Septic	**3.00 (2.25; 3.75)***	**6.00 (5.00; 7.00)**^{*x}	**7.00 (5.00; 8.00)**^{*x}	**5.50 (4.75; 7.25)**^{*x}	**2.50 (2.00; 3.00)***

Table 1. Inflammatory biomarkers, parameters of oxygen dynamics, ROFA scores and components in sham-operated and sepsis groups with different observation periods. Data demonstrate the median and 25th and 75th percentiles. Comparison between groups was conducted with the Kruskal–Wallis test followed by Dunn's post-hoc test. $^{*}P < 0.05$ vs sham-operated groups (in boldface); $^{x}P < 0.05$ vs 12 h sepsis (between sepsis groups) (in boldface).

interval, the ExO_2 values differed significantly from the values of the 12th h septic group ($P_{16h} = 0.035$; $P_{20h} < 0.005$; $P_{24h} = 0.039$).

Time-dependent changes in microhemodynamics

PPV ($P_{16h–28h} < 0.001$; Fig. 2a) and MFI were significantly higher ($P_{16h–28h} < 0.001$; Fig. 2b) as compared with those in the sham-operated group between the 16 and 28 h interval. HI was significantly higher in the 16–28 h time window with a decreasing trend in the septic group, but still being significantly higher compared to the sham-operated group at the 28th h ($P_{28h} = 0.003$; Fig. 2c).

Time-dependent changes in liver mitochondrial functions

OxPhos and $LEAK_{Omy}$ values of septic animals significantly decreased at the 20th h (OxPhos: $P < 0.001$; $LEAK_{Omy}$: $P = 0.006$) compared to the sham-operated group (Fig. 3a,b). CytC%, which characterizes mtOM damage, showed a strong increasing trend with a maximum at the 20th h ($P = 0.028$) and was significantly different from the sham-operated groups between the 16th and the 28th h ($P_{16h–28h} < 0.001$; Fig. 3c). RCR did not differ significantly in the septic animals compared to the sham-operated ones during the whole experimental period (Fig. 3d).

Relative changes in functional parameters over time

The changes in circulatory and mitochondrial parameters as a function of time were examined together with ROFA scores, and significant differences were observed as compared to the sham-operated group. The most marked changes in microcirculatory parameters were observed in the heterogeneity index as an eightfold change between the 16th and 20th h period. Compared to the baseline (12th h), the parameters of the other time points showed the least change in macrocirculation, while more pronounced changes were observed in the ROFA score and mitochondrial parameters (see Supplementary Fig. S2 online).

Receiver operating characteristic (ROC) curve analyses

The diagnostic power of the parameters was determined with the calculated AUC values from the ROC analysis. Among the parameters of ROFA score (Fig. 4a–e), only whole blood lactate level showed relevant predictive value ($AUC_{lactate} = 0.9054$). Among the mitochondrial functions (Fig. 4f–i) CytC% proved to be a strong predictor

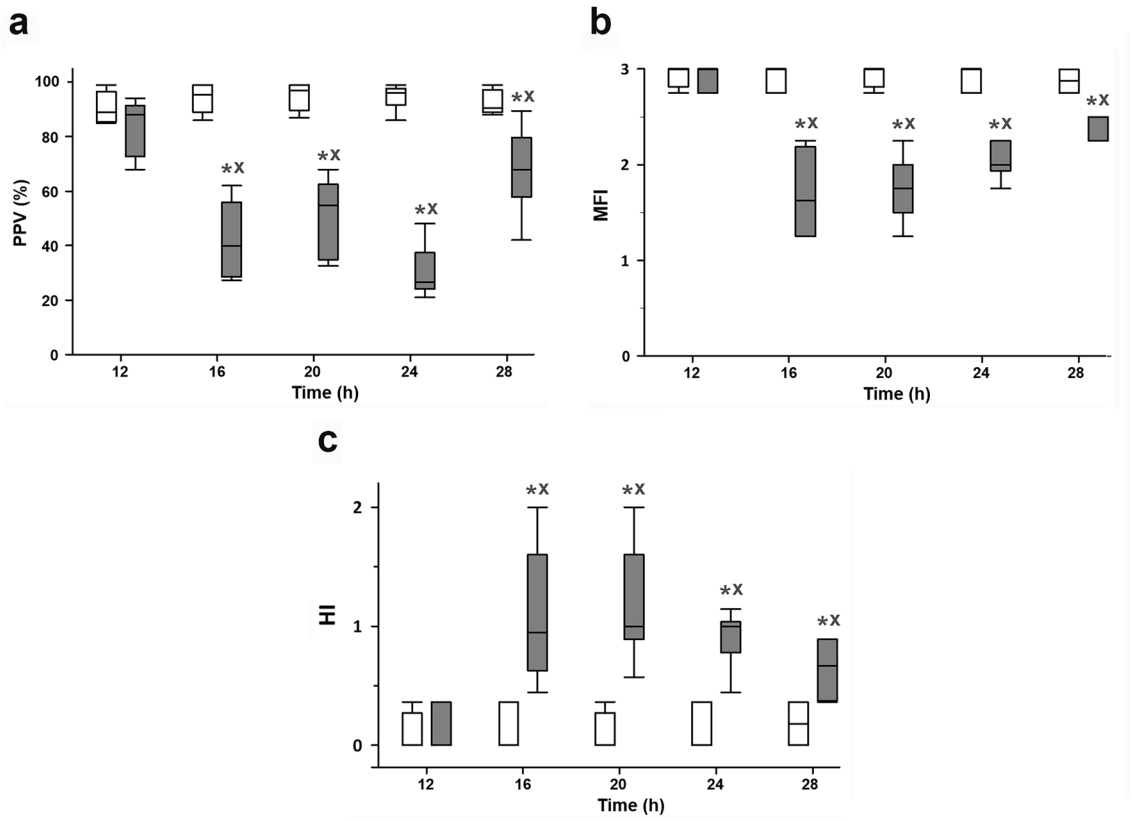

Figure 2. Proportion of perfused vessels (PPV; **a**), microvacular flow index (MFI; **b**) and heterogeneity index (HI; **c**) in the sham-operated animal subgroups (white boxes) and in the sepsis subgroups (grey boxes). The plots demonstrate the median (horizontal line in the box) and the 25th (lower whisker) and 75th (upper whisker) percentiles. Data were analyzed by two-way analysis of variance (ANOVA) followed by the Holm–Sidak post-hoc test. $^{*}P < 0.05$ vs. sham-operated at the same time point, $^{X}P < 0.05$ vs. the 12th h sham-operated group.

($AUC_{CytC\%} = 0.9453$). Among microcirculatory parameters (Fig. 4j–l), PPV showed the strongest diagnostic value ($AUC_{PPV} = 0.9483$), however both MFI and HI had a particularly high diagnostic value ($AUC_{MFI} = 0.8946$; $AUC_{HI} = 0.8851$).

Correlation between mitochondrial and microcirculatory parameters and the ROFA score

There was no significant correlation in the sham-operated groups. There was a negative, significant fair correlation between PPV and the ROFA score ($r = -0.484$, $P = 0.00259$; Fig. 5a) and a positive, significant moderate correlation between HI and the ROFA score ($r = 0.520$, $P = 0.00106$; Fig. 5b). There were no relations between the mitochondrial parameters and the ROFA score (Fig. 5c,d).

Correlation between mitochondrial and microcirculatory parameters

There was no significant correlation in the sham-operated groups. There was no significant correlation between the microcirculation and OxPhos variables (Fig. 6a,b). There was a negative, significant moderate correlation between PPV and CytC% ($r = -0.505$, $P = 0.00153$; Fig. 6c); however, HI and CytC% also showed a moderate and positive relationship ($r = 0.332$, $P = 0.0445$; Fig. 6d).

Discussion

This research protocol was designed to define a possible relationship between microcirculatory and mitochondrial components of the pathobiology of evolving septic reaction as a function of time. The study design strictly adhered to the latest experimental recommendations, and the ensuing septic response followed the expected patterns to reproduce a moderately severe condition. The rodent fecal peritonitis model meets reproducibility and standardization criteria and offers close similarity to a realistic clinical scenario with no source control[8,9,21,22].

Our study presents a hypodynamic model of septic shock since CO declined below the level of the sham-operated group while the increase in CO was observed only at the 16th h. Remarkably, the impaired intestinal microcirculation persists from the start of the study, despite the simultaneous increase in ExO_2, which may indicate sustained cellular metabolic activity. Compared with other findings in the literature, our results are consistent with increased capillary O_2 extraction in early sepsis and emphasize microcirculatory dysfunction as a central component of compromised DO_2[23]. Recent studies also confirm microvascular dysfunction preceding detectable tissue damage[24].

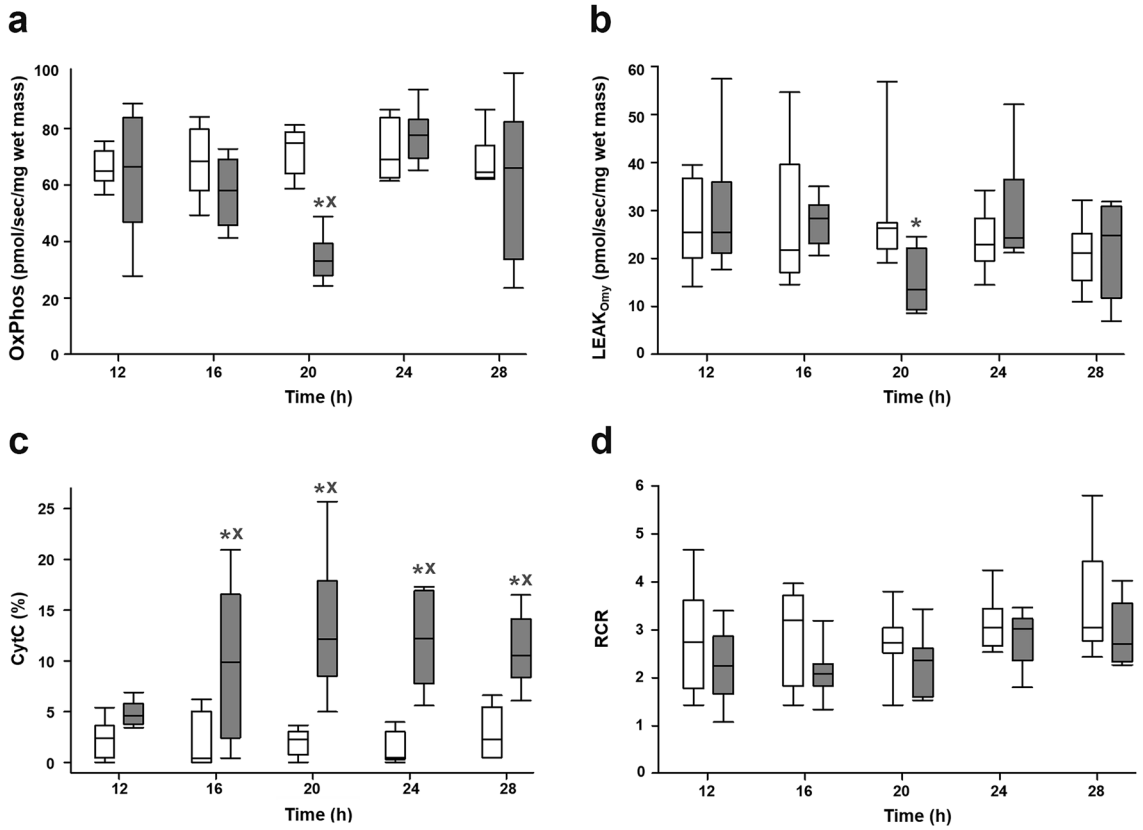

Figure 3. Oxidative phosphorylation (OxPhos; **a**), oligomycin-induced leak state ($LEAK_{Omy}$; **b**), cytochrome c control efficiency (CytC%; **c**) and respiratory control ratio (RCR; **d**) in the sham-operated animal subgroups (white boxes) and in the sepsis subgroups (grey boxes). The plots demonstrate the median (horizontal line in the box) and the 25th (lower whisker) and 75th (upper whisker) percentiles. Data were analyzed by two-way analysis of variance (ANOVA) followed by the Holm–Sidak post-hoc test. $^{*}P<0.05$ vs. sham-operated at the same time point, $^{X}P<0.05$ vs. the 12th h sham-operated group.

In this setup, the divergent dynamics of microcirculatory and mitochondrial responses were clearly discerned with the presence of the whole septic macrohemodynamic pattern with compensatory hyperdynamic, decompensated hypodynamic and final recovery stages which provide insight into the progression of sepsis without resuscitation. The joint feature of microcirculatory-mitochondrial impairment, or MMDS, has already been identified as a significant element in the pathogenesis of human MOF, but alterations to intestinal microcirculation and hepatic mitochondrial functions to date have not been studied together in MOF associated with intraabdominal sepsis[22,25,26]. In theory, a septic insult can affect all of the components of a microcirculatory system, and an increased capillary leakage, glycocalyx damage or intravascular abnormalities can all lead to reduced ExO_2 by the decreased oxygen diffusion and DO_2 within the affected tissues[23,27–30]. Our study partially confirms this notion, showing an early proportionate decrease of perfused microvessels and increased perfusion heterogeneity with matching changes in ROFA scores. Nevertheless, the initial microcirculatory failure was improved and then restored in the later phase of the 28 h observation period. Importantly, the hepatic mitochondrial function deteriorated much later with a rapid recovery of oxidation-linked parameters and a permanently sufficient coupling of the respiratory chain, but CytC% was elevated significantly, implying mtOM damage. CytC is an electron shuttle protein loosely anchored to the mitochondrial inner membrane. Injury to mtOM definitely leads to the partial loss of intramitochondrial CytC and decreased mitochondrial VO_2[31–33]. We have used an established respirometry method to determine mtOM integrity with stimulation of mitochondrial respiration following CytC replacement from an outer source[34,35]. In theory, damage to the mtOM should also involve impairment of mitochondrial coupling, but this was not the case here. CytC% had a high diagnostic power during the whole course of the 28 h experimental period, thus suggesting that it may be a suitable biomarker for the onset of sepsis. However, despite this correlation, CytC% or OxPhos changes did not influence the ROFA score. Our results are consistent with the literature in terms of septic mtOM damage and deterioration of oxidative functions of the respiratory chain. However, the markedly rapid restoration of OxPhos suggests an immense reserve capacity of hepatic mitochondrial respiration to compensate for the loss of membrane integrity. Of note, the correlation between ROFA scores and microcirculatory parameters indicates that the onset of MOF is mainly influenced by microvascular factors, and the correlation between microcirculatory variables and mtOM damage without the involvement of transient loss of oxidative capacities further confirms the presence of strong mitochondrial coping mechanisms against membrane damage.

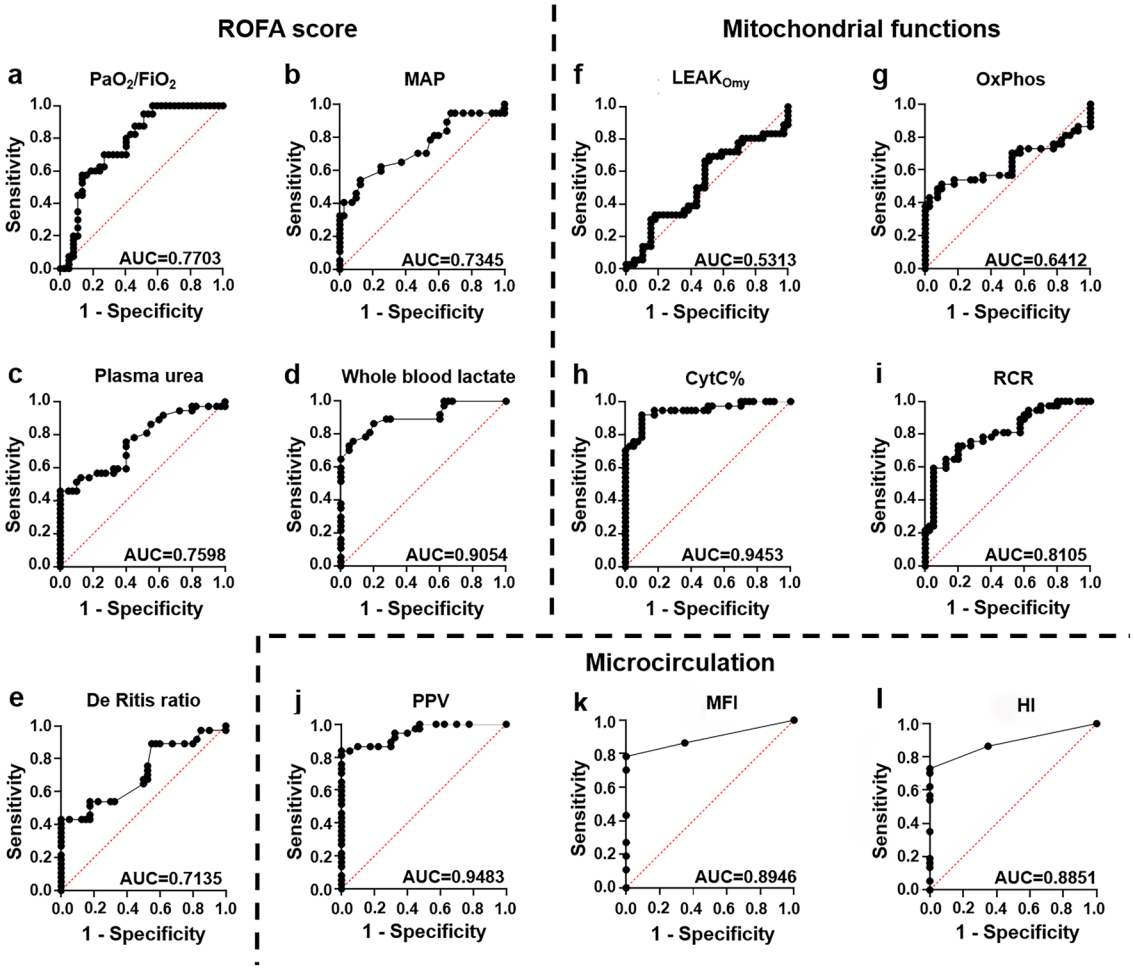

Figure 4. ROC curves provide information about the predictive diagnostic strength of the given parameters. ROC curve of PaO_2/FiO_2 ratio (**a**), mean arterial pressure (MAP; **b**), plasma urea level (**c**), whole blood lactate level (**d**), DeRitis ratio (**e**), oligomycin-induced leak respiration ($LEAK_{Omy}$; **f**), oxidative phosphorylation (OxPhos; **g**), cytochrome c control efficiency (CytC%; **h**), respiratory control ratio (RCR; **i**), proportion of perfused vessels (PPV; **j**), microvascular flow index (MFI; **k**) and heterogeneity index (HI; **l**).

Mitochondrial dysfunction can occur in sepsis both with and without shock as well, but it is not uniformly present. The pathogenesis is complex and still only partially known, but it seems that different mitochondrial functionalities may be present in adjacent areas with microvascular flow heterogeneity[36]. The non-uniformity may also result from the heterogeneous ultrastructural, biophysical and electrochemical characteristics of liver mitochondria, which may lead to potentially decaying and surviving subpopulations in response to pathologies and post-translational processes[37]. Heterogeneity may also arise from the mitochondrial life cycle itself, including biogenesis, motility, fusion and fission, and the clearance of damaged mitochondria. In this line, damaged mitochondria can fuse with other mitochondria with intact membranes, and a regenerative fusion-fission phenomenon was already observed during sepsis progression. Thus, we hypothesize that increased CytC efflux preceded the complete clearance of degraded mitochondria with outer membrane damage and that a structurally and metabolically more resilient and compensatory subpopulation was able to maintain undisturbed ATP synthesis. These mitochondria may be maintainers or restorers of microcirculation and tissue integrity in the later period where sepsis is resolved[38].

In this study design, the ROFA score was used to monitor MOF progression similarly to human clinical routine, and the diagnostic value of microcirculatory parameters could be established within this scheme. As with human practice, the serum lactate level was also significantly elevated and proved to be a strong predictor of severity, supporting the diagnostic importance of hypoxia markers[39]. However, the low ALT, AST and urea levels all point to the direction of "septic stunning", suggesting that the organs were primed with "hypoxic hibernation" for the expected insult.

Braeley et al. have described marked changes in mitochondrial functions[8,9], but microcirculation and MOF have not yet been detected simultaneously. We aimed to complement these measurements by using the latest consensus recommendations, a standardized MOF severity score system and simultaneous microcirculation measurements. Our experimental protocol provided an opportunity to address the chicken or the egg causality dilemma of MMDS in sepsis. Microcirculation is a significantly earlier predictor of multi-organ failure as

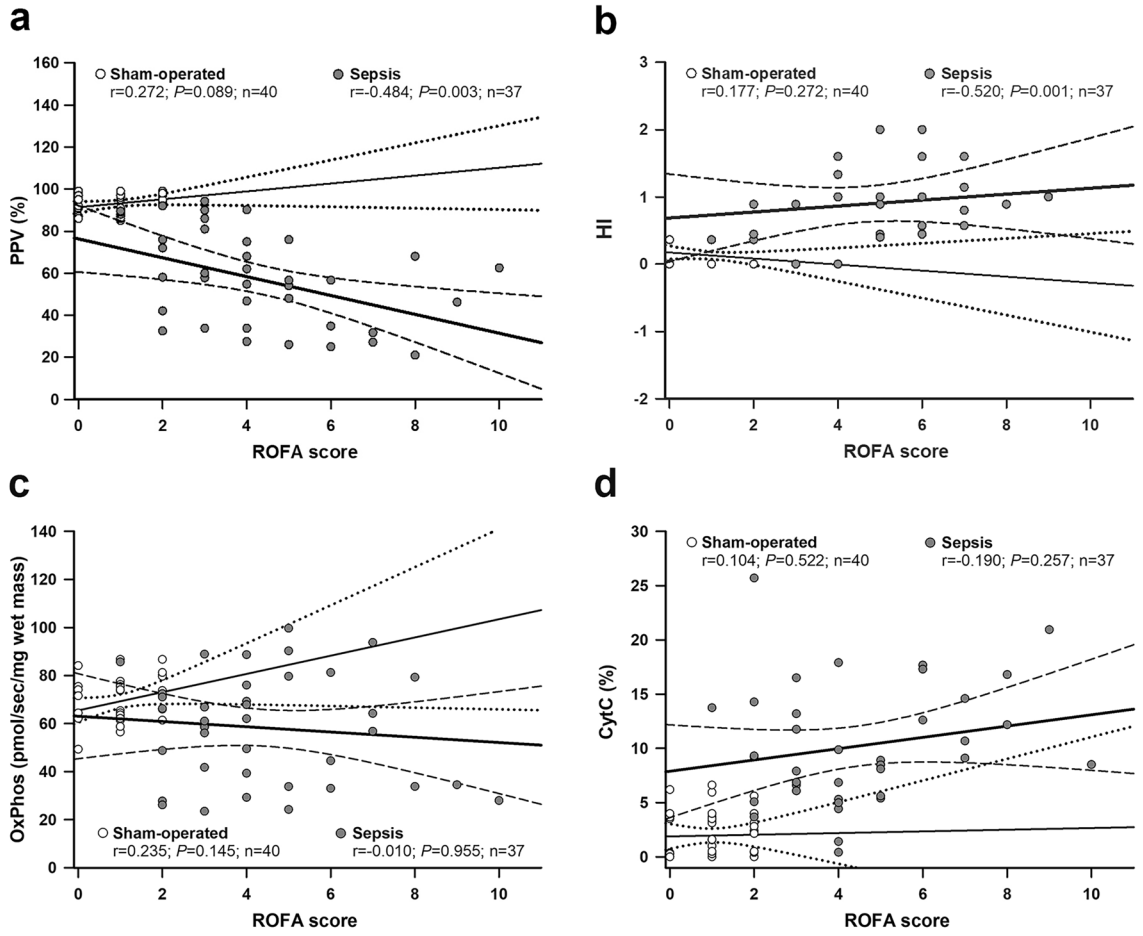

Figure 5. Correlation between the ROFA score and microcirculatory parameters (**a:** proportion of perfused vessels [PPV]; **b:** heterogeneity index [HI]) and mitochondrial functions (**c:** oxidative phosphorylation [OxPhos]; **d:** cytochrome c control efficiency [CytC%]) were examined by the Spearman's correlation test. Correlation coefficient r values, (null hypothesis-related) P values and numbers of animals involved in the sham-operated and septic groups are provided with a 95% confidence interval. The sham-operated subgroup (n = 40) is marked with open circles, a thin regression line and a dotted line for the 95% confidence interval, whereas the septic subgroup (n = 37) is indicated with dark grey circles, a thick regression line and a dashed line for the 95% confidence interval.

compared to mitochondrial respiration. We have used particular parameters to demonstrate that detectable microcirculatory or mitochondrial functional deteriorations occur at different time points depending on the course of sepsis and the compensatory mechanisms and that inappropriate monitoring times may lead to erroneous conclusions. By sequentially tracking the development of MOF, our results shed light on the dynamics of the microvascular oxygen supply, thus providing a better chance for the appropriate timing of diagnostic and therapeutic efforts.

The results demonstrate that an early, marked microcirculatory dysfunction was followed during this time by late and presumably compensatory mitochondrial changes. Our study has certain limitations, which may warrant further investigation. The points of the latest MQTiPSS recommendations were followed, but antibiotics were omitted from the protocol due to their incompletely mapped mitochondrial side effects[40]. In terms of progression, it would have been preferable to allow a longer follow-up. Given the approx. 1:21 ratio of rat time–human time conversion[41], we can assume that the acute phase was fully covered, but additional studies are needed to explore the later effects in later phases of sepsis. Due to the dominant portal blood supply of the liver, the incoming hypoxic signals from the intestines may influence the hepatic mitochondrial functions. Based on this consideration parallel microcirculation and mitochondrial study of the same organ would have been the perfect solution to test our hypothesis, but technical limitations precluded this possibility (intravital videomicroscopy of the liver is influenced by the unique circulation of the sinusoidal structure and the darkness of the tissue itself[42]. Meanwhile, evaluation of intestinal mitochondrial functions is hindered by the high linolenic and oleic acid content, as these molecules can damage the mitochondrial membranes[43]. A future experiment should aim the structural and functional separation of the putative mitochondrial subpopulations could best be investigated in isolated in vitro systems, which did not fit into the present experimental set-up.

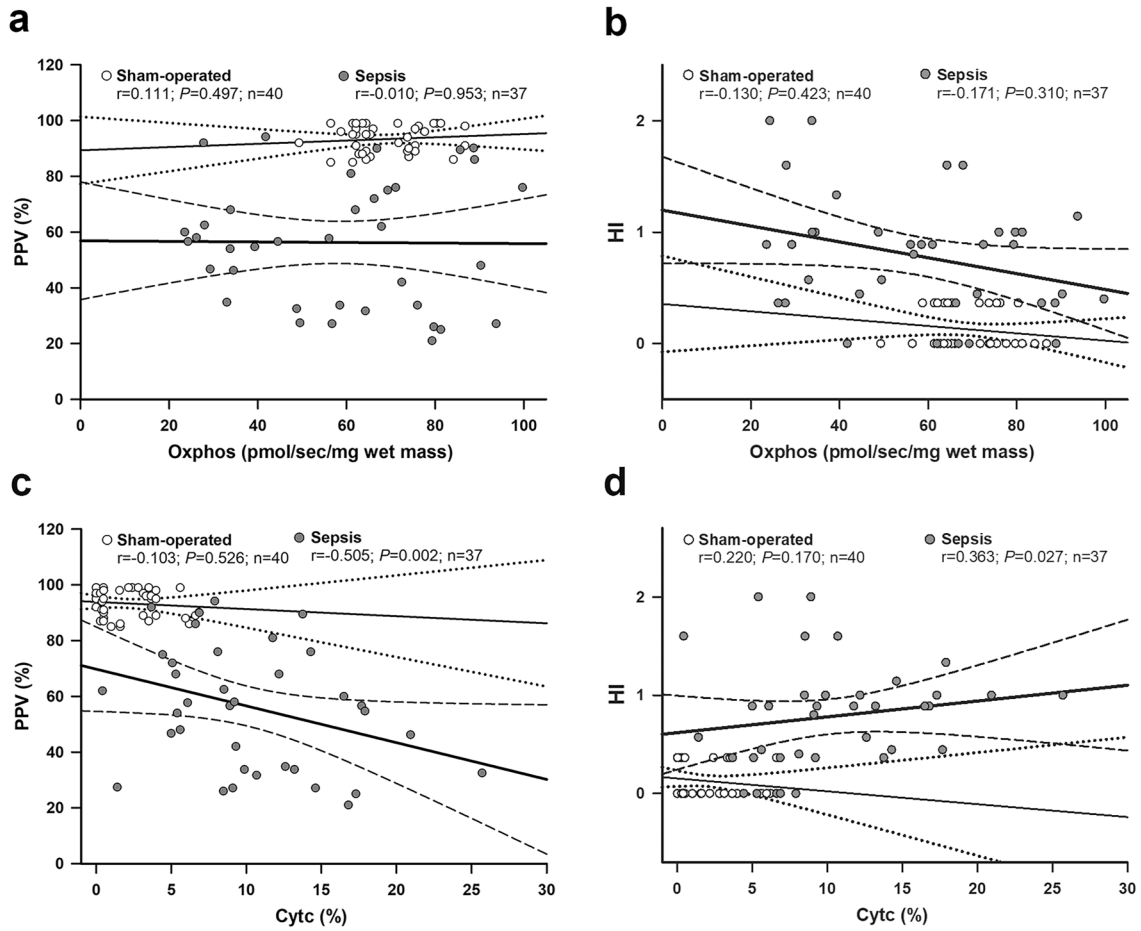

Figure 6. Correlation between oxidative phosphorylation (OxPhos) and proportion of perfused vessels (PPV; **a**) and heterogeneity index (HI; **b**) and between cytochrome c control efficiency (CytC%) and PPV (**c**) and HI (**d**) were examined by the Pearson correlation test. Correlation coefficient r values, (null hypothesis-related) P values and numbers of animals involved in the sham-operated and septic groups are provided with a 95% confidence interval. The sham-operated subgroup (n = 40) is marked with open circles, a thin regression line and a dotted line for the 95% confidence interval, whereas the septic subgroup (n = 37) is indicated with dark grey circles, a thick regression line and a dashed line for the 95% confidence interval.

We designed a rat model of intraabdominal sepsis, and we described the splanchnic microcirculation- and mitochondrial respiration-linked changes in detail with simultaneous tracking. Microvascular perfusion insufficiency proved to be the route of progression and an early predictor of the initiation of MOF. Further, the later decline and rapid recovery of oxidative mitochondrial functions suggest the existence of mitochondrial subpopulations with different responses to tissue hypoxia.

Methods

Animals

Male Sprague–Dawley rats (350 ± 30 g) were housed in plastic cages in a temperature-controlled (21–23 °C) room with a daily 12/12-h light and dark cycle and access to standard rodent food and water ad libitum. Procedures were performed in accordance with NIH guidelines and EU directive 2010/63/EU for the protection of animals used for scientific purposes, and the study was approved by the National Scientific and Ethical Committee, the national competent authority of Hungary. (ETT-TUKEB; license number: V/175/2018).

Sepsis induction and experimental protocol

Sample size was estimated assuming approx. 20% mortality after 24 h. If the presumed true hazard ratio of septic subjects relative to controls is 0.2 with a power of $1-\beta = 0.8$ and the Type I error probability is $\alpha = 0.05$, the inclusion of 8 septic and 8 control animals was recommended for each time point that had been selected. In line with the sample size estimation, the animals were randomly assigned to sham-operated ($n_{\Sigma} = 40$) and septic groups ($n_{\Sigma} = 40$), which were randomly further divided into five independent subgroups each ($n_{12h} = 8$, $n_{16h} = 8$, $n_{20h} = 8$, $n_{24h} = 8$, $n_{28h} = 8$) according to the different time of sepsis progression.

Figure 1a provides a depiction of the experimental protocol. Sepsis was induced with intraperitoneally (ip) administered fecal inoculum, while fresh feces (4 g) samples were collected, filtered and suspended in

physiological saline as described previously[21,44]. Sham-operated animals received the same volume of sterile saline ip. After 6, 12, 16, 20 or 24 h of sepsis progression, the animals received fluid therapy (Ringerfundin, 1.5 mL/kg subcutaneously; B. Braun, Melsungen, Germany) and analgesics (buprenorphine, 15 µg/kg subcutaneously; Richter Pharma, Hungary), and assessments of animal well-being (RSS) was performed. The animals were anesthetized with a mixture of ketamine (45.7 mg/kg) and xylazine (9.12 mg/kg) ip, and invasive hemodynamic monitoring was started after a 30-min stabilization period. The study design and the presentation of the data are in accordance with the Minimum Quality Threshold in Pre-Clinical Sepsis Studies (MQTiPSS) recommendations and considerations[45] and with the Animal Research: Reporting of In Vivo Experiments guidelines (https://arriveguidelines.org/).

Surgical preparation and invasive measurements

The anesthetized animals were placed on a heating pad (37 °C) in a supine position. A tracheostomy was performed to support and provide spontaneous breathing. The right external jugular vein was cannulated for fluid replacement (Ringerfundin, 10 mL/kg/h) and for the maintenance of continuous anesthesia (ketamine 12 mg/kg/h, xylazine 2.4 mg/kg/h and diazepam 0.576 mg/kg/h iv.) during the 60-min monitoring period. The left common carotid artery was cannulated to monitor mean arterial pressure (MAP) and a thermistor-tip catheter was positioned into the contralateral common carotid artery to measure cardiac output (CO) using a thermodilution technique (SPEL Advanced Cardiosys 1.4, Experimetria Ltd., Budapest, Hungary). CO was indexed for body weight. Hemodynamic parameters were measured every 15 min for 60 min. Arterial blood samples were taken for blood gas analyses (Cobas b123; Roche Ltd., Basel, Switzerland) at the 60th min of the monitoring period. The global oxygen delivery ($DO_2 = CO \times [(1.38 \times Hb \times SaO_2) + (0.003 \times PaO_2)]$), oxygen consumption ($VO_2 = CO \times [(1.38 \times Hb \times (SaO_2 - SvO_2)) + (0.003 \times PaO_2)]$) and oxygen extraction ($ExO_2 = DO_2/VO_2$) values were calculated from these parameters. The lung function was determined by using the arterial partial pressure of oxygen to fraction of inspired oxygen (PaO_2/FiO_2, where FiO_2: 0.21) ratio. After the 60-min hemodynamic monitoring period, a median laparotomy was performed to observe the microcirculation of the ileal serosa. A liver tissue biopsy was taken immediately after microcirculatory measurements to evaluate mitochondrial respiratory functions from homogenate. After tissue samplings, animals were sacrificed under deep anesthesia with an overdose of ketamine (120 mg/kg).

Measurements of metabolic, inflammatory and organ dysfunction markers

Whole blood lactate levels were measured from venous blood samples (Accutrend Plus Kit; Roche Diagnostics Ltd., Rotkreuz, Switzerland). Blood samples were collected from the inferior vena cava into EDTA-coated tubes (1 mg/mL), centrifuged (1.200*g* at 4 °C for 10 min) and stored at − 70 °C. Plasma interleukin-6 (IL-6) level was determined according to the standard ELISA kit protocol (Cusabio Biotechnology Ltd., Wuhan, China). Kidney function was characterized by plasma urea level. Liver function was assessed by measuring plasma alanine aminotransferase (ALT) and aspartate aminotransferase (AST) levels using a Roche/Hitachi 917 analyzer (F. Hoffmann-La Roche AG, Switzerland). All analyses were performed in a blinded experimental set-up on coded samples.

Rat organ failure assessment (ROFA) scores

In accordance with the considerations of the Sepsis-3 and MQTiPSS consensus guidelines, the ROFA[21,46] scoring system was used to describe the severity of multiorgan failure. The scoring system considers the cardiovascular (MAP), respiratory (PaO_2/FiO_2 ratio), hepatic (ratio of AST/ALT or De Ritis ratio), renal (urea level) and global metabolic (lactate level) dysfunctions. Sepsis was defined as a cumulative ROFA score over 2.

Microcirculatory measurements

The microcirculation of the ileal serosa was visualized with the Incident Dark Field (IDF) imaging technique (CytoCam Video Microscope System; Braedius Medical, Huizen, the Netherlands) as described earlier[44,46]. The device consists of special LEDs emitting guided light with a wavelength of 530 nm, absorbed by hemoglobin-containing particles, thus the vascular bed appears as a "network of black dots on a grey background". Thanks to the real-time tracking IDF differentiates the rate of blood flow from the movement of the red blood cells[47]. Images from an ileum segment were recorded in six, 50-frame, high-quality video clips. The records were analyzed with an offline software-assisted system (AVA 3.0, Automated Vascular Analysis, Academic Medical Center, University of Amsterdam). The proportion of perfused vessels (PPV) was defined as the ratio of the perfused vessel lengths to total vessel lengths: (total number of vessels—[no flow + intermittent flow]/total number of vessels) × 100[48]. Microvascular flow index (MFI) was randomly and blindly determined by a single researcher. After a semiquantitative analysis by eye, individual vessels were distinguished between no flow (0), intermittent flow (1), sluggish flow (2), and continuous flow (3). A value was assigned to each vessel and the overall score of each record was the average of the individual values. The heterogeneity index (HI) was defined as the difference between the highest MFI and the lowest MFI divided by the average MFI of the record: $(MFI_{highest} - MFI_{lowest})/MFI_{average}$[46,49,50]. The equation used in calculating the microvascular parameters is shown in Supplementary Equation S1.

Assessment of liver mitochondrial function

Mitochondrial VO_2 ($mtVO_2$) was measured in liver homogenates using High-Resolution FluoRespirometry (Oxygraph-2 k, Oroboros Instruments, Innsbruck, Austria) as described earlier[44]. In brief, liver samples obtained from the left lateral lobe were homogenized with a tissue grinder Potter–Elvehjem, and then respirometry was performed in a MiR05 respiration medium at constant temperature and with continuous stirring (37 °C, 750 rpm). After stabilization of O_2 consumption, rotenone was added (1) to inhibit complex I activity and (2) to prevent

accumulation of oxaloacetate (a known endogenous inhibitor of complex II). $FADH_2$-supported leak respiration and maximal capacity of oxidative phosphorylation (OxPhos) were determined in the presence of succinate and adenosine diphosphate (ADP). Following stimulation of OxPhos, the integrity of the mitochondrial outer membrane (mtOM) was tested with the addition of exogenous cytochrome c, and the increase in $mtVO_2$ was expressed as a percentage of $mtVO_2$ as compared to $mtVO_2$ in OxPhos (CytC%). Complex V (or ATP synthase) was inhibited by oligomycin to assess leak respiration in a non-phosphorylating state ($LEAK_{Omy}$) and to calculate respiratory control ratio (RCR), an index of the coupling of mitochondrial respiration to OxPhos (Oxphos/$LEAK_{Omy}$). DatLab 7.3.0.3. Software (Oroboros Instruments, Innsbruck, Austria) was used for online display, respirometry data acquisition and analysis.

Statistical analysis

Data were evaluated with the SigmaStat 13 software package (Systat Software, San Jose, CA). Survival rate was analyzed and plotted using the Kaplan–Meier method. The Mann–Whitney or Kruskal–Wallis tests were used with Dunn's post-hoc test for discrete (score) variables, while a two-way analysis of variance was used for continuous variables followed by the Holm–Sidak post-hoc test. Data were displayed as median values and interquartile ranges between the 75th and 25th percentiles, with $P < 0.05$ being considered significant. The receiver operating characteristic (ROC) curve analysis was used to evaluate the classification power to represent the diagnostic accuracy of the different parameters. A multivariate analysis model was performed with a logical data analysis method and data processing with GraphPad Prism 8.0 software. Pearson's method (for the ROFA score) or Spearman's methods were used to analyze linear correlation; correlation coefficient (r), regression lines and 95% confidence intervals were indicated.

Data availability

The datasets generated during and/or analyzed during the current study are available from the corresponding author on reasonable request.

Received: 21 August 2023; Accepted: 22 March 2024
Published online: 26 March 2024

References

1. Singer, M. *et al.* The third international consensus definitions for sepsis and septic shock (sepsis-3). *J. Am. Med. Assoc.* **315**, 801–810 (2016).
2. Ince, C. The microcirculation is the motor of sepsis. *Crit. Care.* **9**, 13–19 (2005).
3. Mongardon, N., Dyson, A. & Singer, M. Is MOF an outcome parameter or a transient, adaptive state in critical illness?. *Curr. Opin. Crit. Care.* **15**, 431–436 (2009).
4. De Backer, D. *et al.* Microcirculatory alterations in patients with severe sepsis: Impact of time of assessment and relationship with outcome. *Crit. Care. Med.* **41**, 791–799 (2013).
5. Moore, J. P. R., Dyson, A., Singer, M. & Fraser, J. Microcirculatory dysfunction and resuscitation: Why, when, and how. *Br. J. Anaesth.* **115**, 366–375 (2015).
6. Balestra, G. M., Legrand, M. & Ince, C. Microcirculation and mitochondria in sepsis: Getting out of breath. *Curr. Opin. Anaesthesiol.* **22**, 184–190 (2009).
7. Jarczak, D., Kluge, S. & Nierhaus, A. Sepsis-pathophysiology and therapeutic concepts. *Front. Med. Lausanne.* **8**, 628302. https://doi.org/10.3389/fmed.2021.628302 (2021).
8. Brealey, D. *et al.* Mitochondrial dysfunction in a long-term rodent model of sepsis and organ failure. *Am. J. Physiol. Regul. Integr. Comp. Physiol.* **286**, 491–497 (2004).
9. Mesquida, J. *et al.* Prognostic implications of tissue oxygen saturation in human septic shock. *Intensive Care Med.* **38**, 592–597 (2012).
10. Sakr, Y., Dubois, M. J., De Backer, D., Creteur, J. & Vincent, J. L. Persistent microcirculatory alterations are associated with organ failure and death in patients with septic shock. *Crit. Care Med.* **32**, 1825–1831 (2004).
11. Spronk, P.E. Microcirculatory and Mitochondrial Distress Syndrome (MMDS): A New Look at Sepsis. in *Functional Hemodynamic Monitoring: Update in Intensive Care and Emergency Medicine.* (ed. Pinsky, M.R., Payen, D.) 47–67 (Springer, 2005).
12. Clowes, G. H., O'Donelli, T. F. & Ryan, N. T. Energy metabolism in sepsis: Treatment based on different patterns in shock and high output stage. *Ann. Surg* **179**, 684–694 (1974).
13. Lang, C. H., Bagby, G. J., Ferguson, J. L. & Spritzer, J. J. Cardiac output and redistribution of organ blood flow in hypermetabolic sepsis. *Am. J. Physiol.* **246**, 331–337 (1984).
14. Protti, A. & Singer, M. Bench-to-bedside review: Potential strategies to protect or reverse mitochondrial dysfunction in sepsis-induced organ failure. *Crit. Care.* **10**, 228. https://doi.org/10.1186/cc5014 (2006).
15. Singer, M., De Santis, V., Vitale, D. & Jeffcoat, W. Multiorgan failure is an adaptive, endocrine-mediated, metabolic response to overwhelming systemic inflammation. *Lancet.* **364**, 545–548 (2004).
16. Standage, S. W. *et al.* PPARα augments heart function and cardiac fatty acid oxidation in early experimental polymicrobial sepsis. *Am. J. Physiol. Heart. Circ. Physiol.* **312**, 239–249 (2017).
17. Preau, S. Energetic dysfunction in sepsis: A narrative review. *Ann. Intensive. Care.* **11**, 104. https://doi.org/10.1186/s13613-021-00893-7 (2021).
18. Brealey, D. *et al.* Association between mitochondrial dysfunction and severity and outcome of septic shock. *Lancet.* **360**, 219–223 (2002).
19. Kohoutová, M., Dejmek, J. & Tůma, Z. Variability of mitochondrial respiration in relation to sepsis-induced multiple organ dysfunction. *Physiol. Res.* **67**, 577–592 (2018).
20. Donati, A. *et al.* From macrohemodynamic to the microcirculation. *Crit. Care. Res. Pract.* **2013**, 892710. https://doi.org/10.1155/2013/892710 (2013).
21. Tallósy, S. P. *et al.* The microbial composition of the initial insult can predict the prognosis of experimental sepsis. *Sci. Rep.* **11**, 22772. https://doi.org/10.1038/s41598-021-02129-x (2021).
22. Bauer, M. *et al.* Mortality in sepsis and septic shock in Europe, North America and Australia between 2009 and 2019—Results from a systematic review and meta-analysis. *Crit. Care.* **24**, 239. https://doi.org/10.1186/s13054-020-02950-2 (2020).
23. Ellis, C. G., Bateman, R. M., Sharpe, M. D., Sibbald, W. J. & Gill, R. Effect of a maldistribution of microvascular blood flow on capillary O(2) extraction in sepsis. *Am. J. Physiol. Heart Circ. Physiol.* **282**, 156–164 (2002).

24. Kowalewska, P. M. *et al.* Spectroscopy detects skeletal muscle microvascular dysfunction during onset of sepsis in a rat fecal peritonitis model. *Sci. Rep.* **12**, 6339. https://doi.org/10.1038/s41598-022-10208-w (2022).
25. Clark, J. A. & Coopersmith, C. M. Intestinal crosstalk: A new paradigm for understanding the gut as the "motor" of critical illness. *Shock.* **28**, 384–393 (2007).
26. Nakajima, Y., Baudry, N., Duranteau, J. & Vicaut, E. Microcirculation in intestinal villi: A comparison between hemorrhagic and endotoxin shock. *Am. J. Respir. Crit. Care. Med.* **164**, 8. https://doi.org/10.1164/ajrccm.164.8.2009065 (2001).
27. Mammen, E. F. The haematological manifestations of sepsis. *J. Antimicrob. Chemother.* **41**, 17–24 (1998).
28. Iba, T. & Levy, J. H. Sepsis-induced coagulopathy and disseminated intravascular coagulation. *Anesthesiology.* **132**, 1238–1245 (2020).
29. Spronk, P. E., Zandstra, D. F. & Ince, C. Bench-to-bedside review: Sepsis is a disease of the microcirculation. *Crit. Care.* **8**, 462–468 (2004).
30. Sullivan, R. C., Rockstrom, M. D., Schmidt, E. P. & Hippensteel, J. A. Endothelial glycocalyx degradation during sepsis: Causes and consequences. *Matrix Biol. Plus.* **12**, 100094. https://doi.org/10.1016/j.mbplus.2021.100094 (2021).
31. Borutaite, V., Budriunaite, A., Morkuniene, R. & Brown, G. C. Release of mitochondrial cytochrome c and activation of cytosolic caspases induced by myocardial ischaemia. *Biochim. Biophys. Acta.* **1537**, 101–109 (2001).
32. Andersen, L. W. *et al.* Cytochrome C in patients with septic shock. *Shock.* **45**, 512–517 (2016).
33. Adachi, N. *et al.* Serum cytochrome c level as a prognostic indicator in patients with systemic inflammatory response syndrome. *Clin. Chim. Acta.* **342**, 127–136 (2004).
34. Kay, L., Daneshrad, Z. & Saks, V. A. Alteration in the control of mitochondrial respiration by outer mitochondrial membrane and creatine during heart preservation. *Cardiovasc. Res.* **34**, 547–556 (1997).
35. Eleftheriadis, T., Pissas, G., Liakopoulos, V. & Stefanidis, I. Cytochrome c as a potentially clinical useful marker of mitochondrial and cellular damage. *Front. Immunol.* **7**, 279. https://doi.org/10.3389/fimmu.2016.00279 (2006).
36. Ince, C. & Mik, E. G. Microcirculatory and mitochondrial hypoxia in sepsis, shock, and resuscitation. *J. Appl. Physiol.* **120**, 226–235 (2016).
37. Ngo, J., Osto, C., Villalobos, F. & Shirihai, O. S. Mitochondrial heterogeneity in metabolic diseases. *Biology (Basel).* **10**, 927. https://doi.org/10.3390/biology10090927 (2021).
38. Chen, H., Chomyn, A. & Chan, D. C. Disruption of fusion results in mitochondrial heterogeneity and dysfunction. *J. Biol. Chem.* **280**, 26185–26192 (2005).
39. Zhai, X. *et al.* Lactate as a potential biomarker of sepsis in a rat cecal ligation and puncture model. *Mediators Inflamm.* **2018**, 8352727. https://doi.org/10.1155/2018/8352727 (2018).
40. Suárez-Rivero, J. M. *et al.* Mitochondria and antibiotics: For good or for evil?. *Biomolecules.* **11**, 1050. https://doi.org/10.3390/biom11071050 (2021).
41. Sengupta, P. The laboratory rat: Relating its age with human's. *Int. J. Prev. Med.* **4**, 624–630 (2013).
42. Uz, Z. *et al.* Intraoperative imaging techniques to visualize hepatic (micro)perfusion: An overview. *Eur. Surg. Res.* **61**, 2–13 (2020).
43. Stanbury, P. J. Comparison of the mitochondria of the small intestine of vertebrates. *Nature.* **192**, 67. https://doi.org/10.1038/192067a0 (1961).
44. Rutai, A. *et al.* Endothelin A and B receptors: Potential targets for microcirculatory-mitochondrial therapy in experimental sepsis. *Shock.* **54**, 87–95 (2019).
45. Osuchowski, M. F. *et al.* Minimum quality threshold in pre-clinical sepsis studies (MQTiPSS): An international expert consensus initiative for improvement of animal modeling in sepsis. *Shock.* **50**, 377–380 (2018).
46. Juhász, L. *et al.* Divergent effects of the N-methyl-D-aspartate receptor antagonist kynurenic acid and the synthetic analog SZR-72 on microcirculatory and mitochondrial dysfunction in experimental sepsis. *Front. Med. Lausanne.* **27**, 566582. https://doi.org/10.3389/fmed.2020.566582 (2020).
47. Aykut, G., Veenstra, G., Scorcella, C., Ince, C. & Boerma, C. Cytocam-IDF (incident dark field illumination) imaging for bedside monitoring of the microcirculation. *Intensive Care Med Exp.* **3**, 40. https://doi.org/10.1186/s40635-015-0040-7 (2015).
48. De Backer, D., Creteur, J., Preiser, J. C., Dubois, M. J. & Vincent, J. L. Microvascular blood flow is altered in patients with sepsis. *Am. J. Respir. Crit. Care Med.* **166**, 98–104 (2002).
49. Ince, C. *et al.* Second consensus on the assessment of sublingual microcirculation in critically ill patients: Results from a task force of the European Society of Intensive Care Medicine. *Intensive Care Med.* **44**(3), 281–299 (2018).
50. Pozo, M. O., Kanoore Edul, V. S., Ince, C. & Dubin, A. Comparison of different methods for the calculation of the microvascular flow index. *Crit. Care Res. Pract.* **2012**, 102483. https://doi.org/10.1155/2012/102483 (2012).

Acknowledgements

This research was conducted with the support of the University of Szeged Open Access Fund (Grant Number: 6475) and by Grant No. EFOP-3.6.2-16-2017-00006.

Author contributions

R.F. and Sz.P.T. conceived and wrote the manuscript. J.K., A.Sz. and M.B. supervised and administered the investigation and critically reviewed the manuscript. A.R. and R.F. performed sepsis induction and handled in vivo part of the experiments. R.F. performed microcirculatory measurements and analyzed the videoclips. L.J. was involved in the mitochondrial measurements. R.F. and Sz.P.T. performed statistical analysis of data and constructed the figures. A.Sz. and M.P. critically checked the consistency of the figures.

Funding

Open access funding provided by University of Szeged.

Competing interests

The authors declare no competing interests.

Additional information

Supplementary Information The online version contains supplementary material available at https://doi.org/10.1038/s41598-024-57855-9.

Correspondence and requests for materials should be addressed to M.B. or S.P.T.